

#	TITLE	PRESENTER
1	Model wavefunctions for an interface between lattice Laughlin and Moore-Read states	Blazej Jaworowski
2	A random unitary circuit model for black hole evaporation	Christoph Sunderhauf
3	AKLT-states as ZX-diagrams: diagrammatic reasoning for quantum states	Richard D.P.East
4	Anderson complexes: Bound states of atoms due to Anderson localization	Krzysztof Giergiel
5	Continuous matrix product operator approach to finite temperature quantum states	Wei Tang
6	Correlation-enhanced Neural Networks as Interpretable Variational Quantum States	Agnes Valenti
7	Efficient MPS methods for extracting spectral information on rings and cylinders	Maarten Van Damme
8	Generating Function for Tensor Network Diagrammatic Summation	Wei-Lin Tu
9	Homogeneous Floquet time crystal from weak ergodicity breaking	Hadi Yarloo
10	Horizon bound in QFT	Ivan Kukuljan
11	Investigation of the Néel phase of the frustrated Heisenberg antiferromagnet by differentiable symmetric tensor networks	Juraj Hasik
12	Measurement-induced transition in random quantum circuits: from stroboscopic to continuous	M. Szyniszewski
13	Non-separable time-crystal structures on the Mobius strip	Arkadiusz Kuros
14	Resonating valence bond realization of spin-1 non-Abelian chiral spin liquid on the torus	Hua-Chen Zhang
15	Simulation of three-dimensional quantum systems with projected entangled-pair states	Patrick Vlaar
16	Solving frustrated Ising models using tensor networks	Bram Vanhecke
17	String order parameters for symmetry fractionalization in an enriched toric code	Mohsin Iqbal
18	The SYK model from strained honeycomb irridates: A case study	Mikael Fremling
19	Variational wave functions for spin-phonon models	F. Ferrari

Model wavefunctions for an interface between lattice Laughlin and Moore-Read states

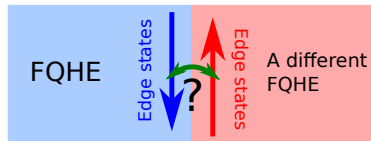
Blazej Jaworowski

Model wavefunctions for interfaces between lattice Laughlin and Moore-Read states

Błażej Jaworowski, Anne E.B. Nielsen

Motivation: What happens at non-Abelian FQH interfaces?

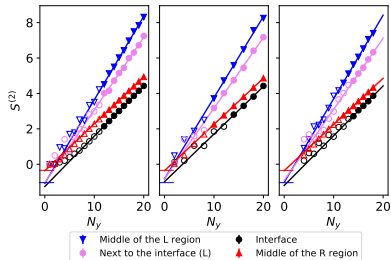
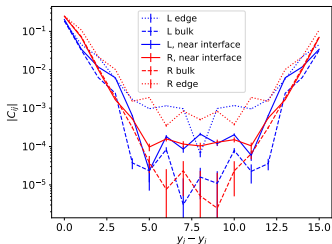
- ▶ Interfaces can have topological structure which can generate nontrivial phenomena (e.g. additional topological degeneracy).
- ▶ Few microscopic works – ED is hard. Model wavefunctions can help.
- ▶ Almost all of them describe continuum systems
- ▶ Anyons are important, but we are not aware of any microscopic studies.



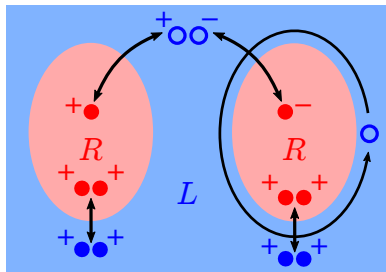
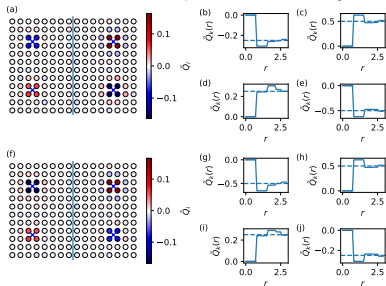
Method: Model wavefunctions from CFT correlator of two types of vertex operators,

$$\Psi(\mathbf{n}) = \langle 0 | \prod_{i=1}^{N_L} V_{i,\text{MR}}(z_i, n_i) \prod_{i=N_L+1}^N V_{i,\text{Laughlin}}(z_i, n_i) | 0 \rangle ,$$

and Monte Carlo study of their properties (GS+quasiholes+quasielectrons).



► **Ground state:** particle density, correlation function, entanglement entropy



► **Anyons:** charge and statistics of anyons before and after crossing the interface.

► **Multiple islands:** topological degeneracy.

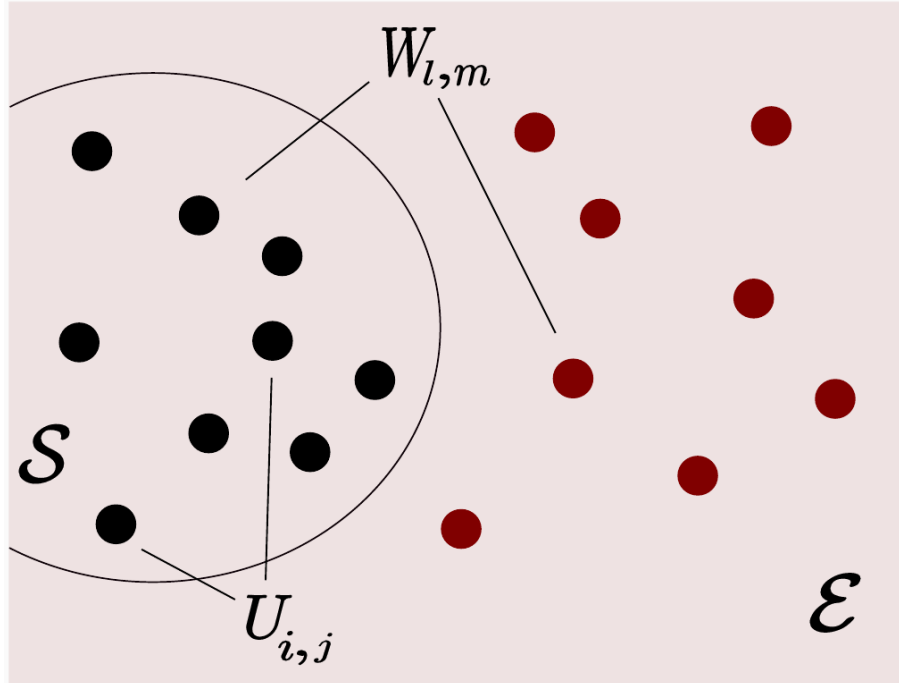
A random unitary circuit model for black hole evaporation

Christoph Sunderhauf

A random unitary circuit model for black hole evaporation

Lorenzo Piroli*, Christoph Sünderhauf*, Xiao-Liang Qi (* contributed equally)

JHEP 2020: 63 (2020), arXiv: 2002.09236



Coupling to environment

$W_{l,m}$ SWAP

Intrinsic dynamics

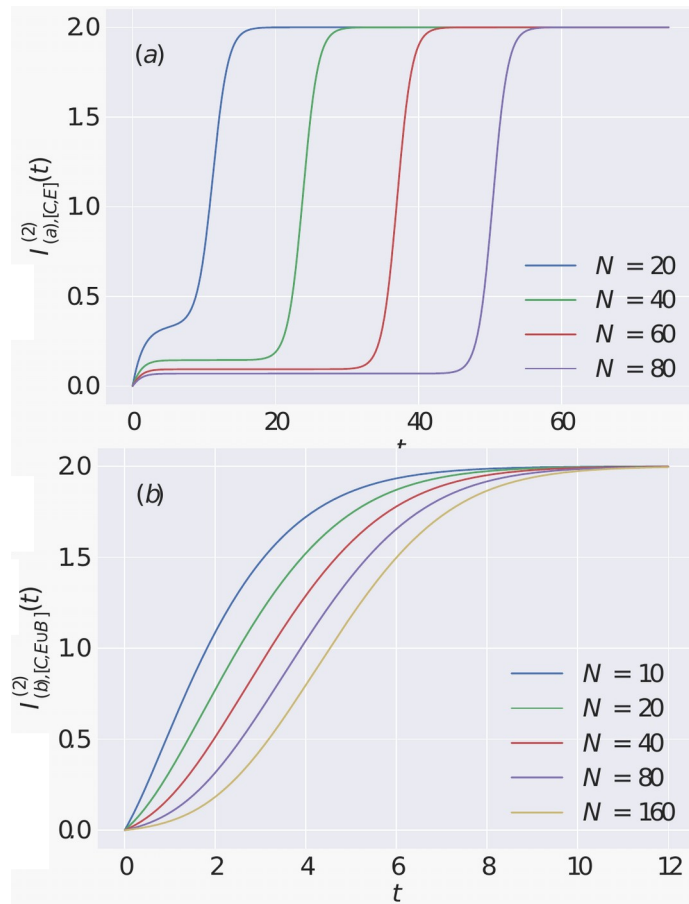
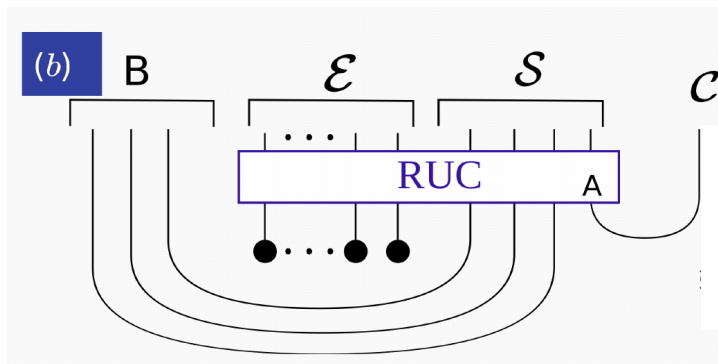
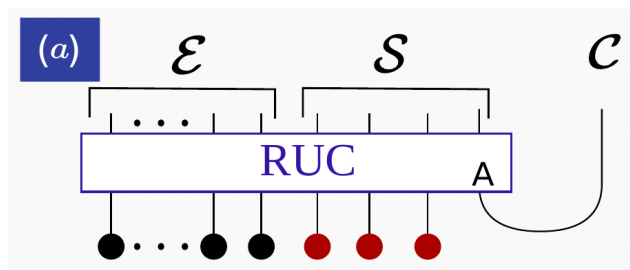
$U_{i,j}$ Haar-random

(w/ & w/o charge conservation)

A random unitary circuit model for black hole evaporation

Lorenzo Piroli*, Christoph Sünderhauf*, Xiao-Liang Qi (* contributed equally)

JHEP 2020: 63 (2020), arXiv: 2002.09236



AKLT-states as ZX-diagrams: diagrammatic reasoning for quantum states

Richard D.P.East

AKLT-states as ZX-diagrams: diagrammatic reasoning for quantum states

Richard D. P. East, John van de Wetering, Nicholas Chancellor, and Adolfo G. Grushin, arXiv:2012.01219.

- Tensor networks have found numerous applications.
- They are an excellent graphical representation of states.

But

- Diagrammatic representations of tensor networks are an excellent aid, but not a calculation tool.

Our solution

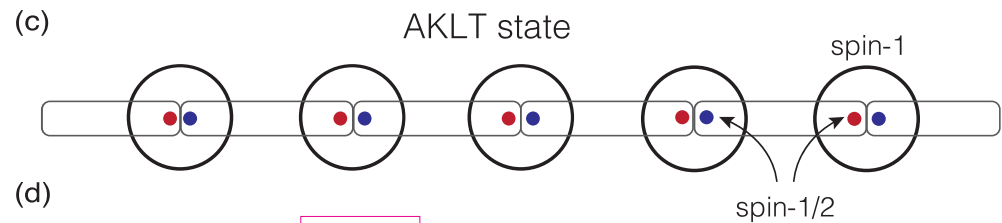
- The ZX calculus is a diagrammatic language for qubit tensor networks.
- We can perform calculations by *only* altering the diagrams.

(a) Singlet $\begin{array}{|c|} \hline \bullet \quad \bullet \\ \hline \end{array} = \frac{1}{\sqrt{2}} (|01\rangle - |10\rangle) \propto \begin{array}{c} \pi \\ \pi \end{array}$

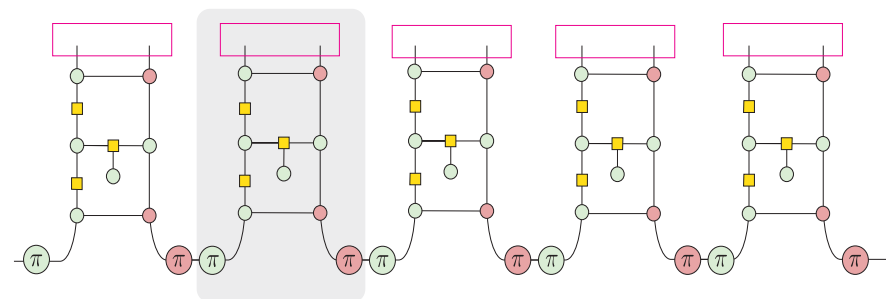
(b) Projector $\begin{array}{|c|} \hline \bullet \quad \bullet \\ \hline \end{array} = |+\rangle \langle 11| + |0\rangle \frac{\langle 10| + \langle 01|}{\sqrt{2}} + |-\rangle \langle 00|$
 \propto

(e) MPS equivalence

$\propto M^{[n]+1}$ $\propto M^{[n]0}$ $\propto M^{[n]-1}$



(f)



Things you can do

- In the 1D AKLT state we identify the edge states, retrieve the MPS representation, and prove the existence of a string order diagrammatically.
- In 2D we simplify the proof that the 2D AKLT state is a universal resource.

$$\begin{aligned}
 & \frac{1}{2} \begin{array}{c} \text{Diagram 1: A 2x2 grid of nodes. Top row: red, red. Middle row: green, green. Bottom row: green, red. Edges: horizontal and vertical. Yellow squares on vertical edges between middle and bottom rows. Green circles labeled } \pi \text{ on bottom edges.} \end{array} \stackrel{(\pi \mathbf{c})}{=} \frac{1}{2\sqrt{2}} \begin{array}{c} \text{Diagram 2: Similar to Diagram 1, but with green circles labeled } \pi \text{ on bottom edges.} \end{array} \stackrel{(\mathbf{c})}{=} \frac{1}{2\sqrt{2}} \begin{array}{c} \text{Diagram 3: Similar to Diagram 2, but with red circles labeled } \pi \text{ on bottom edges.} \end{array} \\
 & \stackrel{(\text{ex})}{=} \frac{1}{2} \begin{array}{c} \text{Diagram 4: A green circle labeled } \pi \text{ on the left, a red circle labeled } \pi \text{ on the right, connected by a horizontal edge. A green circle is above the left } \pi \text{ circle.} \end{array} \stackrel{(\mathbf{c})}{=} \frac{1}{2} \begin{array}{c} \text{Diagram 5: A red circle labeled } \pi \text{ on the left, a red circle labeled } \pi \text{ on the right, connected by a horizontal edge. A green circle is above the left } \pi \text{ circle.} \end{array} \stackrel{(\mathbf{f})}{=} \begin{array}{c} \text{Diagram 6: A red circle labeled } \pi \text{ on the left, a red circle labeled } \pi \text{ on the right, connected by a horizontal edge.} \end{array} \\
 & = 2 \begin{pmatrix} 0 & 0 \\ 1 & 0 \end{pmatrix} = \frac{1}{\sqrt{6}} M^{[n]+1}
 \end{aligned}$$

Example of a diagrammatic calculation.

Anderson complexes: Bound states of atoms due to Anderson localization

Krzysztof Giergiel

Anderson Complexes - Why?

- Cold atomic system driven by time periodic external force can give rise to **time crystals**.
- Disordered time periodic driving gives rise to **Anderson localization in time domain**.
- Cold atoms by **Feshbach** resonance give control over interaction strength (even sign).
- It is natural to investigate **periodic driving** of internal **interaction strength** instead of external force.
- If this interaction strength varies in disordered fashion in time what will we see?

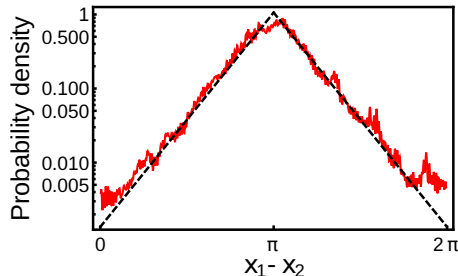
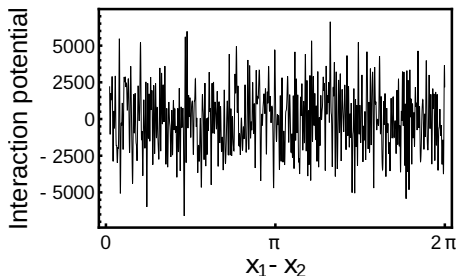
What?

Anderson Complexes - Bound states of atoms due to Anderson localization

$$H = \frac{p_{12}^2}{m^*} + V(r_{12}),$$

$V(r_{12})$ is a random function with infinite support.

In localized regime one expect exponential localization in relative distance:

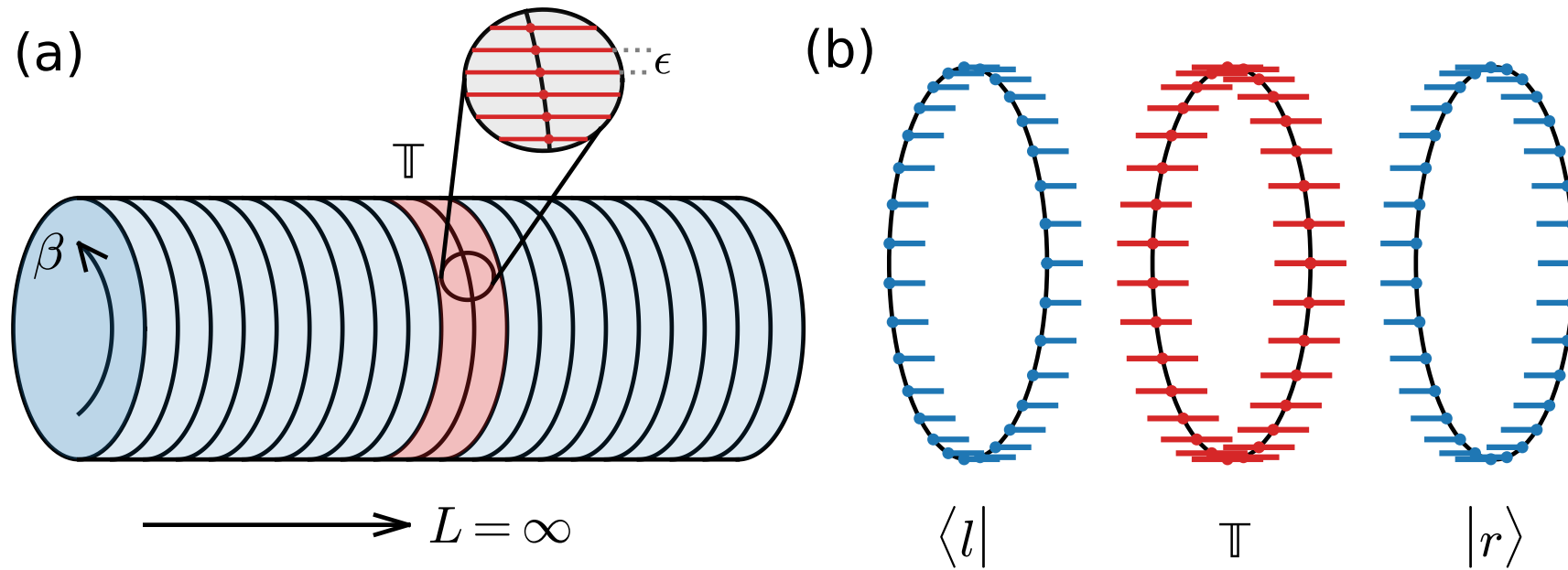


Continuous matrix product operator approach to finite temperature quantum states

Wei Tang

CONTINUOUS MATRIX PRODUCT OPERATOR APPROACH TO FINITE TEMPERATURE QUANTUM STATES

Wei Tang @ PKU

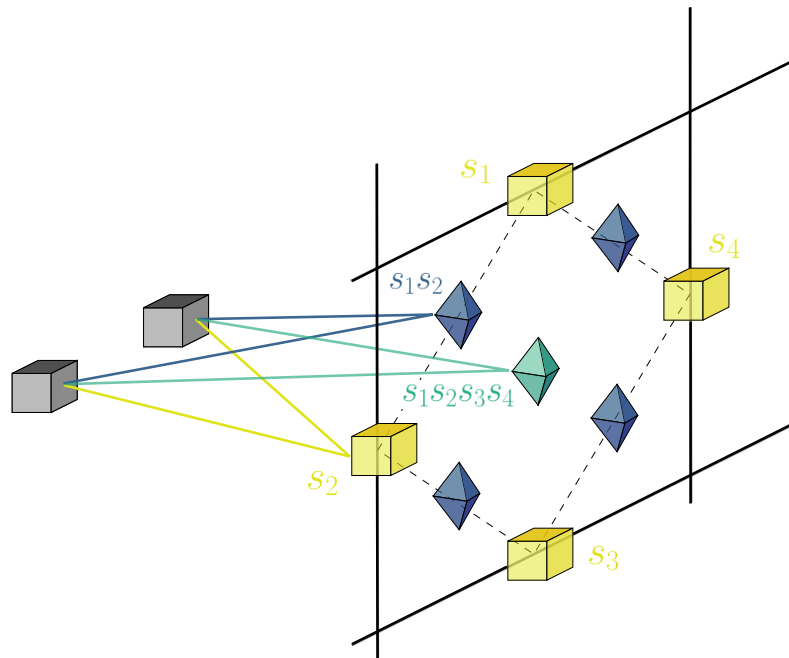


Correlation-enhanced Neural Networks as Interpretable Variational Quantum States

Agnes Valenti

Correlation-enhanced Neural Networks as Variational Quantum States

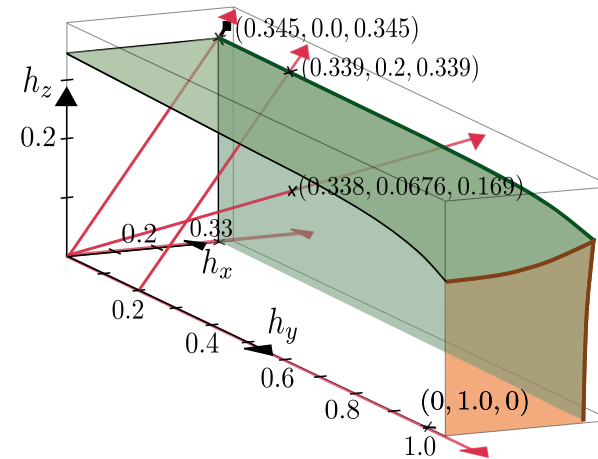
RBM with correlators



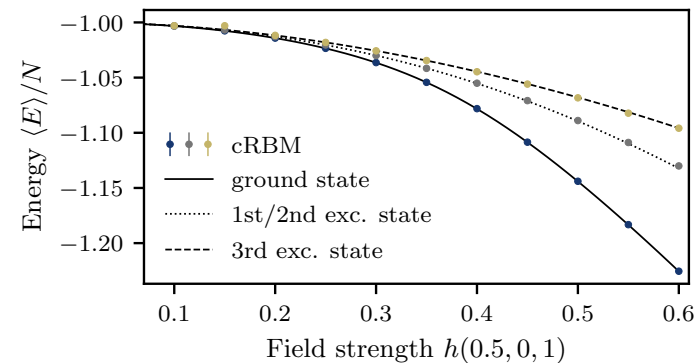
In preparation:

A Valenti (ETH Zürich), E Greplova, NH Lindner and SD Huber

Topological phases



Excited states without symmetries



Efficient MPS methods for extracting spectral information on rings and cylinders

Maarten Van Damme

Efficient MPS methods for extracting spectral information on rings and cylinders

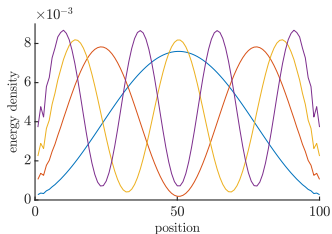
Quasiparticle ansatz

$$\sum_i A_1^l \text{---} \dots \text{---} B_i \text{---} \dots \text{---} A_N^r \quad (1)$$

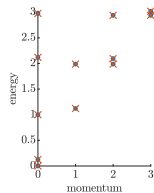
Applied to

- ▶ finite mps
- ▶ cylinder infinite mps

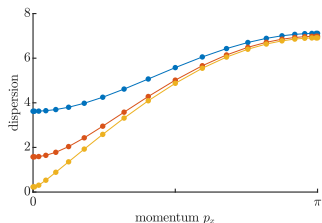
Efficient MPS methods for extracting spectral information on rings and cylinders



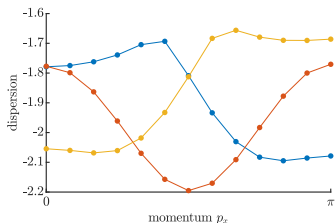
(a) spin 1 heisenberg, OBC



(b) critical ising, PBC



(c) cylinder ising, $p_y = 0$



(d) Magnon hubbard, different p_y

Generating Function for Tensor Network Diagrammatic Summation

Wei-Lin Tu

GENERATING FUNCTION FOR TENSOR NETWORK DIAGRAMMATIC SUMMATION

Wei-Lin Tu

Institute for Solid State Physics(ISSP), University of Tokyo

WT, H.-K. Wu, N. Schuch, N. Kawashima, and J.-Y. Chen, arXiv:2101.03935 (2021)

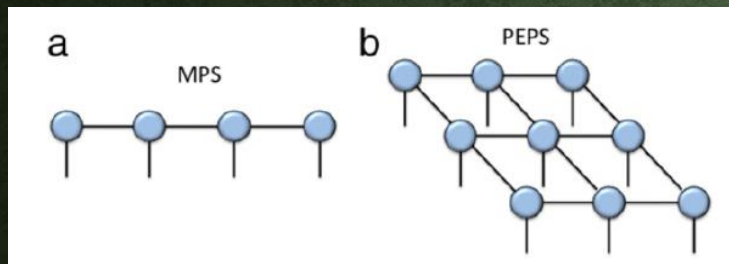
wtu@issp.u-tokyo.ac.jp



Benasque Entanglement in Strongly
Correlated Systems @ zoom
2021/02/23



Tensor Networks:



R. Orus, Annals of Physics 349, 117-158 (2014).

Generating
function



$$|G_{\Phi}(\lambda)\rangle = \text{C} \left[\text{blue square} \right]_{s_1} \text{---} \left[\text{blue square} \right]_{s_2} \text{---} \left[\text{blue square} \right]_{s_3} \text{---} \dots \text{---} \left[\text{blue square} \right]_{s_{N-1}} \text{---} \left[\text{blue square} \right]_{s_N} \text{C}$$

$$MPS_j(\lambda) = A + \lambda e^{-ikr_j} B$$

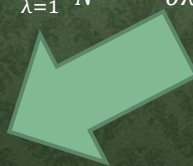
$$\hat{G}_{SF}(\lambda) = \text{white circle with } \hat{O}^\alpha \text{ --- red circle} \text{ --- red circle} \text{ ---} \dots \text{--- red circle} \text{ --- red circle}$$

$s_1 \quad s_2 \quad s_3 \quad \dots \quad s_{N-1} \quad s_N$

One-particle excitation:

$$|\Phi_k(B)\rangle = \sum_{j=0}^{N-1} e^{-ikj} \hat{T}^j \text{C} \left[\text{white square } B \right]_{s_1} \text{---} \left[\text{white square } A \right]_{s_2} \text{---} \dots \text{---} \left[\text{white square } A \right]_{s_N} \text{C}$$

$$\frac{\partial |G_{\Phi}(B, \lambda)\rangle}{\partial B} \Big|_{\substack{B=0, \\ \lambda=1}} \frac{1}{N} < \frac{\partial \hat{G}_{SF}(\lambda)}{\partial \lambda} \Big|_{\lambda=0} >$$



$$\hat{O}_j^\beta(\lambda) = I + \lambda e^{-ikr_j} \hat{O}^\beta$$

Static structural factor:

$$S^{\alpha, \beta}(k) = \frac{1}{N} \sum_{j, j'=1}^N e^{ik \cdot (r_j - r_{j'})} \langle \hat{O}_j^\alpha \hat{O}_{j'}^\beta \rangle$$

*With the help of desired generating functions,
the number of tensors under consideration
can be largely reduced!*

Homogeneous Floquet time crystal from weak ergodicity breaking

Hadi Yarloo

Horizon bound in QFT

Ivan Kukuljan

Horizon bound in QFT

- Prepare a QFT in a short range correlated initial state $\langle O(x)O(y) \rangle_C \propto e^{-|x-y|/\xi}$

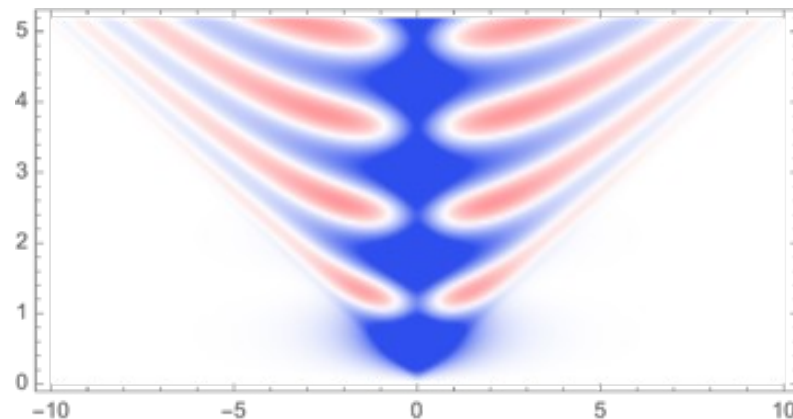
- Quench $H_0 \rightarrow H$

- Correlations spread within a horizon

$$|\langle O(t, x)O(t, y) \rangle_C| < \kappa e^{-\max\{(|x-y|-2ct)/\xi_h, 0\}}$$

- Proven in CFT, demonstrated analytically and numerically in many systems, observed experimentally

→ Believed to be a general property of quantum systems



Horizon violation

- Oscillating infinite range correlations of currents

$$C_\mu(t, x, y) = \langle J^\mu(t, x) J^\mu(t, y) \rangle$$

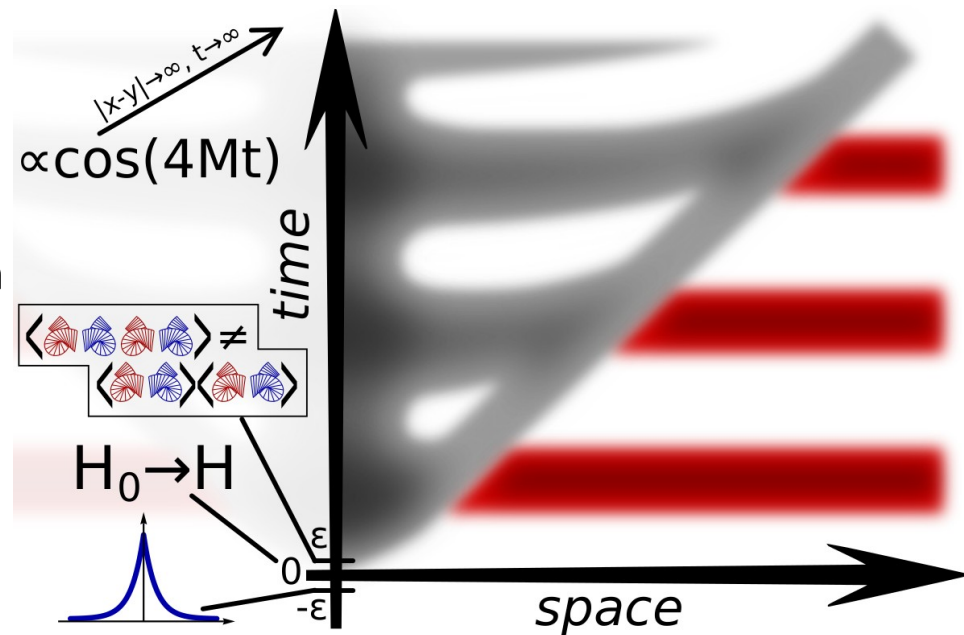
- Found in the **sine-Gordon model** (using bosonisation and truncated Hamiltonian methods)

IK, Sotiriadis, Takács, JHEP 2020, 224

- Recently found in gauge theory – **1+1D quantum electrodynamics** (using THM)

IK, arXiv:2101.07807 [hep-th]

- Related to nontrivial field topology



Investigation of the Néel phase of the frustrated Heisenberg antiferromagnet by differentiable symmetric tensor networks

Juraj Hasik

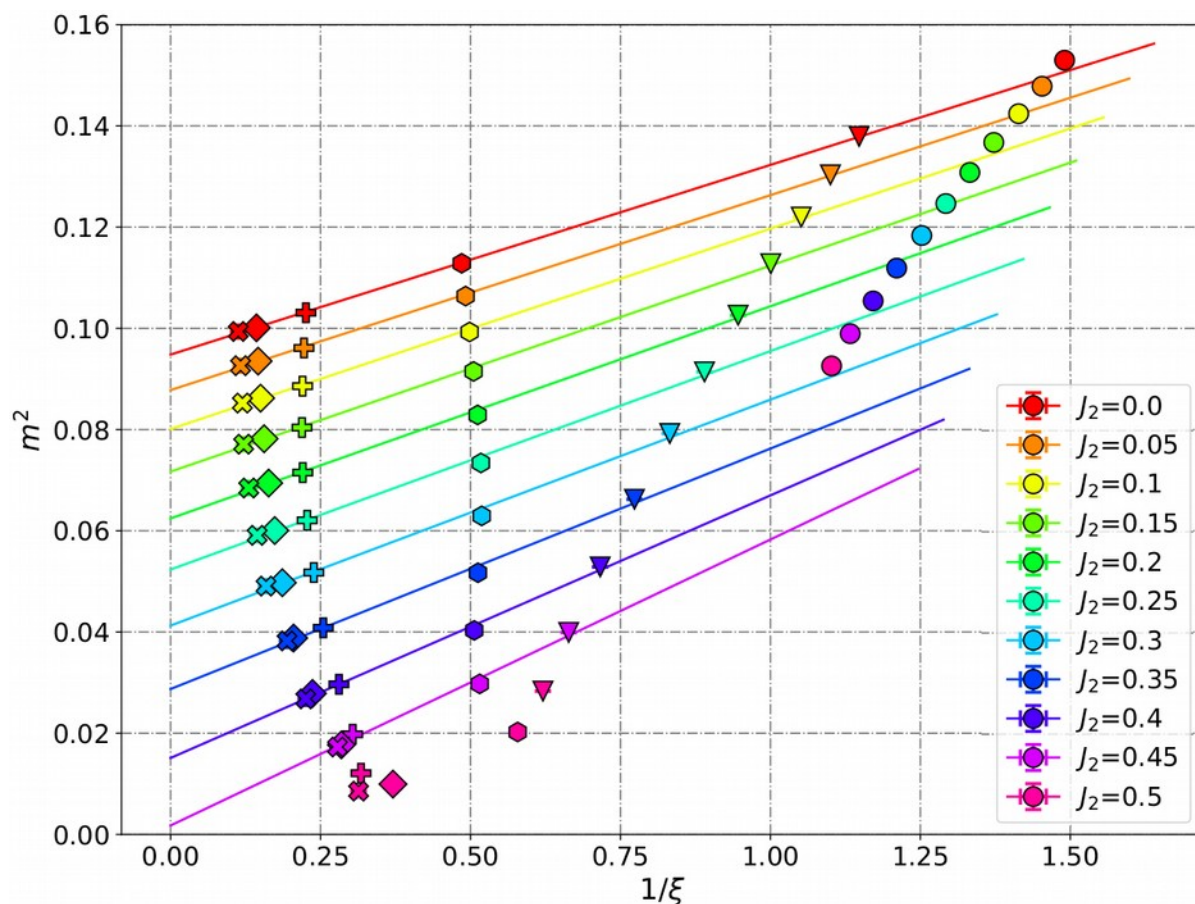
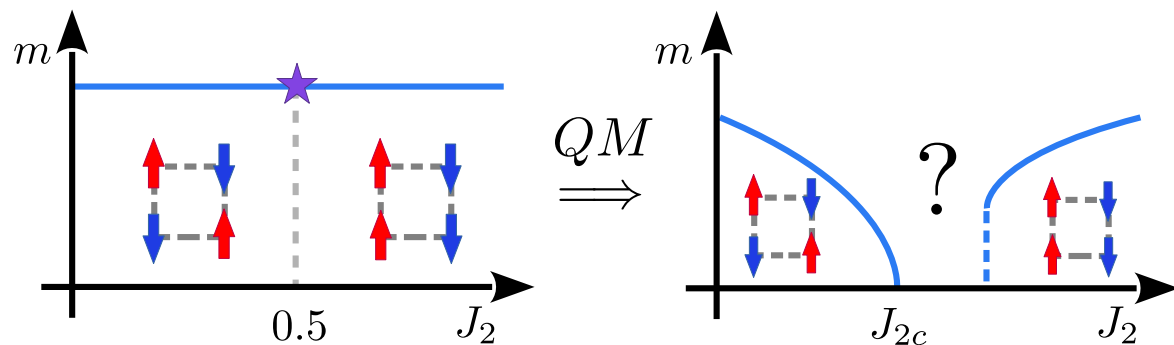
HOW TO iPEPS: The case of J1-J2

Juraj Hasik, Federico
Becca, Didier Poilblanc

I. Gradient based
optimization with AD

II. Extract symmetry
structure

III. Analyze with finite
correlation-length
scaling



**Investigation of the Néel phase of the frustrated Heisenberg antiferromagnet
by differentiable symmetric tensor networks, *SciPost Phys.* 10, 012 (2021)**

Measurement-induced transition in random quantum circuits: from stroboscopic to continuous

M. Szyniszewski

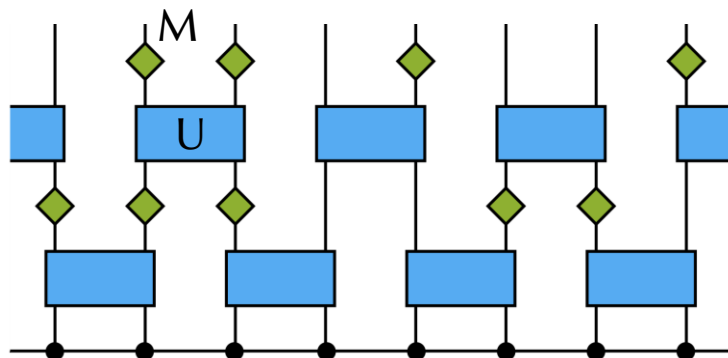
Measurement-induced transition in random quantum circuits: from stroboscopic to continuous

BY M. SZYNISZEWSKI, A. ROMITO, H. SCHOMERUS

Phys. Rev. B 100, 064204 (2019) & Phys. Rev. Lett. 125, 210602 (2020)

Quantum circuit

- Random unitary evolution (U) and weak measurements (M)

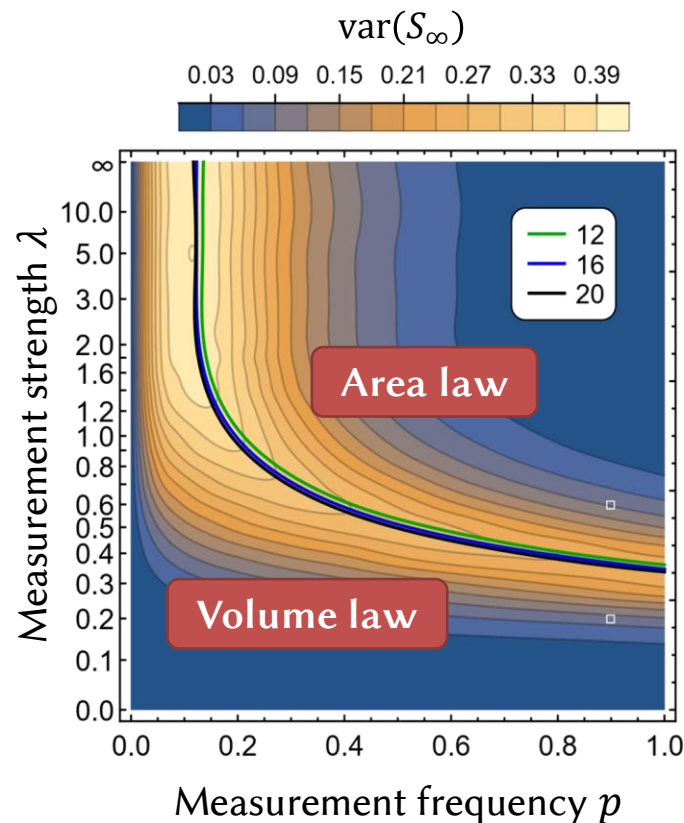


- What is the stationary state entanglement?

U favours volume law.

M (if strong) favours area law.

Stroboscopic measurements: phase diagram

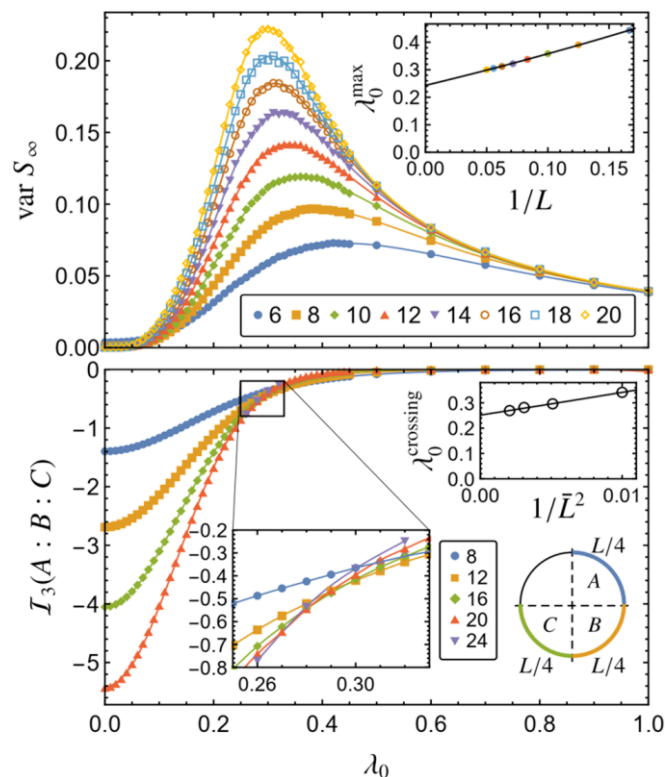


BY M. SZYNISZEWSKI, A. ROMITO, H. SCHOMERUS

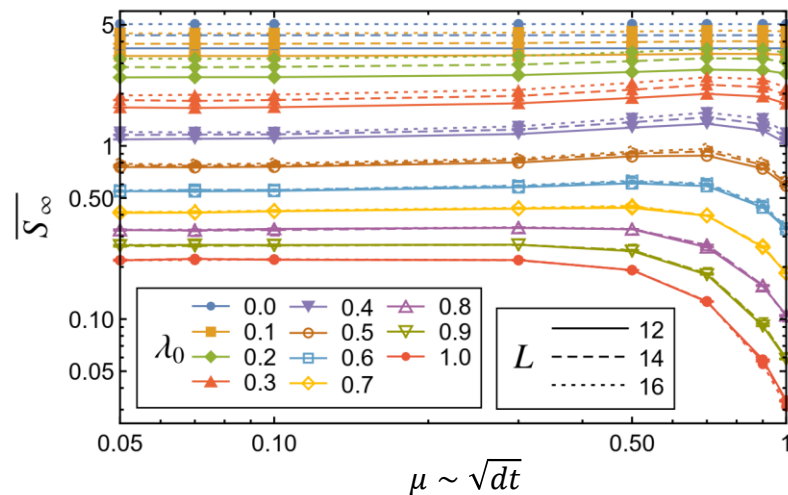
Phys. Rev. B 100, 064204 (2019) & Phys. Rev. Lett. 125, 210602 (2020)

Continuous measurements: phase transition

- Phase transition still present when continuous measurement is used



Universality of the phase transition



Discrete and continuous regimes seem to be smoothly connected and exhibit similar critical exponents. Universality between the two regimes?

Non-separable time-crystal structures on the Mobius strip

Arkadiusz Kuros

Non-separable time-crystal structures on the Möbius strip

Krzysztof Giergiel¹
 Arkadiusz Kuroś¹
 Arkadiusz Kosior²
 Krzysztof Sacha¹

¹Institute of Theoretical Physics, Jagiellonian University in Kraków, Poland
²Max-Planck-Institut für Physik Komplexer Systeme, Dresden, Germany



Abstract

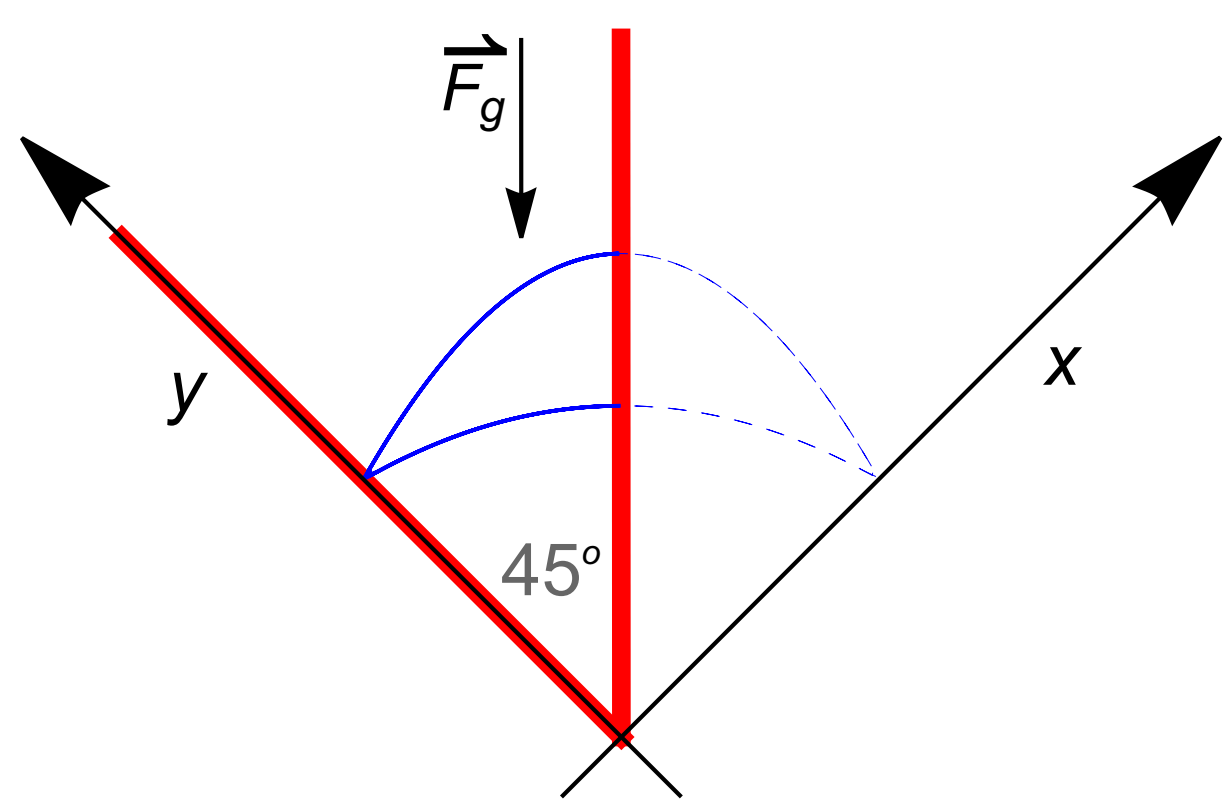
Periodically driven many-body quantum systems provide a comfortable platform for modelling crystalline structure in the time dimension which opens a path to realize temporal condensed matter physics and explore novel phenomena. It has been already shown that the time domain can host Anderson localization, Mott insulator phase [1], topological phases [2], dynamical phase transitions [3], quasi-crystals [4] and fractional time crystals [5].

Here, we present a simple implementation of non-separable two-dimensional lattices with a non-trivial topology in the time domain that can be created for a Bose-Einstein condensate bouncing resonantly between two oscillating mirrors. As an example, we consider a three-band Lieb lattice [6] on the Möbius strip with a middle flat band. The dynamics of the flat band is governed solely by interactions, which can be easily tuned by periodic changes of scattering length using Feshbach resonance mechanism. This allows us to engineer exotic long-range interactions [7] and offers a new perspective for studying exotic many-body dynamics.

Single-particle bouncing between two oscillating mirrors

- Hamiltonian in the frame oscillating with the mirrors

$$H = \frac{p_x^2 + p_y^2}{2} + x + y + (x + y)f_y(t) + yf_{y-x}(t) \quad y \geq x \geq 0$$



the mirrors are located around $x = 0$ and $x - y = 0$ and form a wedge with the angle 45°

- $H(t) = H(t + T) \quad T = \frac{2\pi}{\omega}$
- $f_y(t)$, $f_{y-x}(t)$ - periodic functions correspond to the mirror oscillations

The static wedge for $f_y(t) = f_{y-x}(t) = 0$

- wedge with the angle 90°

- the system is integrable \rightarrow action-angle variables

$$H_0(I_x, I_y) = \frac{(3\pi)^{2/3}}{2} (I_x^{2/3} + I_y^{2/3}) \quad \theta_{x,y} = \Omega_{x,y}t + \theta_{x,y}(0) \quad \Omega_{x,y}(I_x, I_y) = \frac{dH_0(I_x, I_y)}{dI_{x,y}}$$

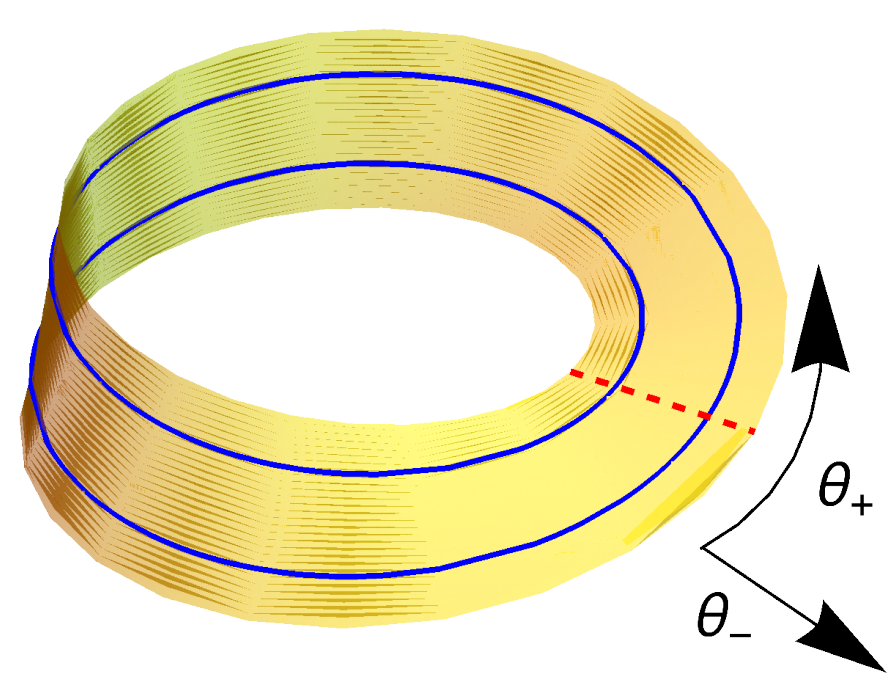
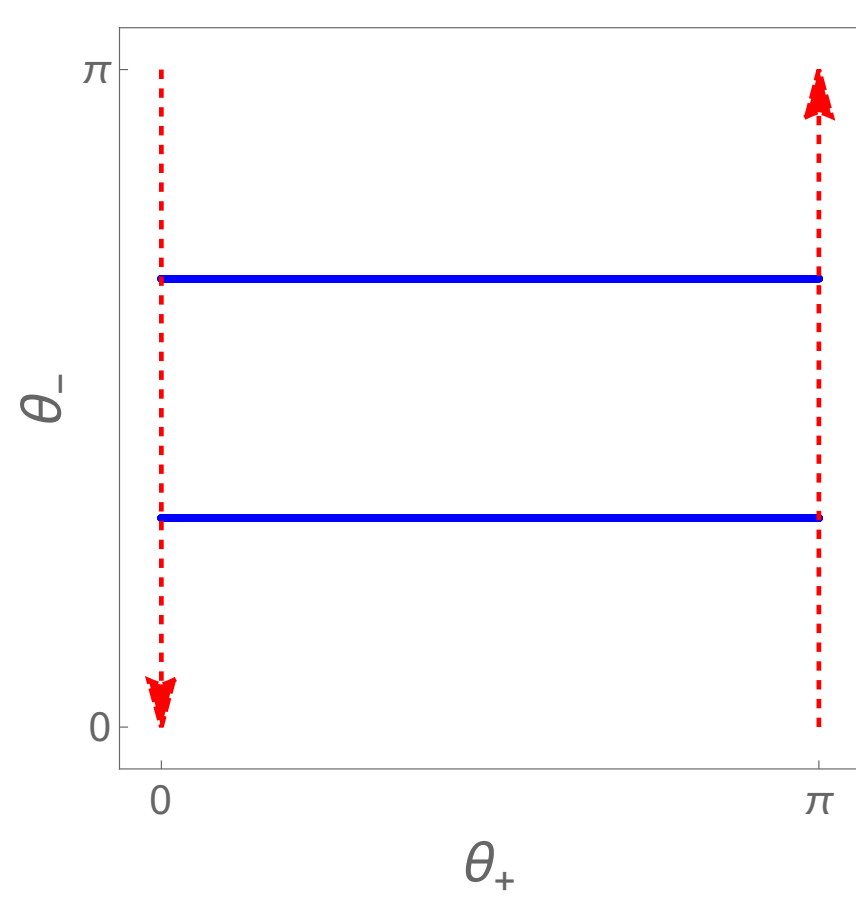
- for $k_x \Omega_x(I_x) = k_y \Omega_y(I_y)$

- all trajectories are periodic
- third independent integral of motion $I_\theta = (k_y \theta_y - k_x \theta_x) \pmod{2\pi}$
- periodic orbit can be described by a single frequency only
- canonical transformation from $(I_x, I_y, \theta_x, \theta_y)$ to new variables $(I_+, I_-, \theta_+, \theta_-)$

$$I_\pm = \text{const} \quad \theta_- = \text{const} \quad \theta_+ = \Omega t + \theta_+^0$$

- wedge with the angle 45° for $k_x = k_y$

$$\dot{I}_\pm = \dot{\theta}_\pm = 0 \quad \dot{\theta}_+ = \Omega_+(I_+) \quad \text{with} \quad \{\theta_+ = \pi, \theta_-\} = \{\theta_+ = 0, \pi - \theta_-\}$$



Periodically oscillating mirrors

- resonant driving of a particle $\omega = s\Omega_+(I_+^0, I_-^0)$ s – integer number
- classical secular approximation
- canonical transformation to the frame moving along a resonant orbit

$$\Theta_+ = \theta_+ - \Omega_+ t \quad \Theta_- = \theta_- \quad P_\pm = I_\pm - I_\pm^0$$

- Cartesian coordinates $x(I_\pm, \Theta_\pm)$ and $y(I_\pm, \Theta_\pm)$ can be expanded in the Fourier series

$$x, y = \sum_{n=-\infty}^{\infty} c_n^{x,y}(I_+, \Theta_-) e^{in(\Omega_+ t + \Theta_+)}$$

- all dynamical variables evolve slowly if we choose initial conditions close to the resonant orbits
- averaging over the fast time variable
- effective time-independent Hamiltonian that describes the motion of a particle close to a resonant orbit

$$\mathcal{H}_{\text{eff}} = \langle H \rangle_t = \frac{P_-^2 + P_+^2}{2m_{\text{eff}}} + V_{\text{eff}}(\Theta_\pm, f_y, f_{y-x}) \quad \{\Theta_+ = \pi, \Theta_-\} = \{\Theta_+ = 0, \pi - \Theta_-\}$$

By different shaking protocols of two mirrors i.e. $f_y(t)$ and $f_{y-x}(t)$, it is feasible to construct many lattice geometries, just like in optical lattice engineering.

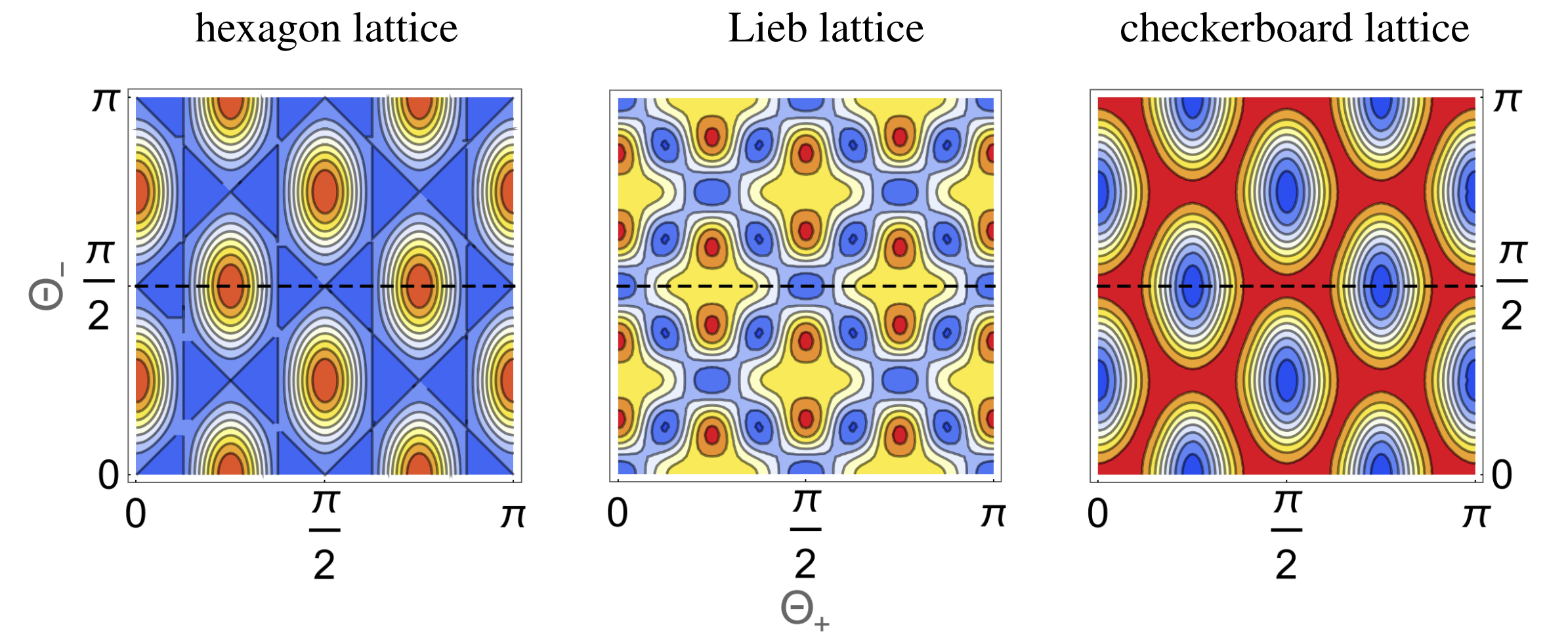
Lattice structures

- effective Hamiltonian

$$H_{\text{eff}} = \frac{P_-^2 + P_+^2}{2m_{\text{eff}}} - \frac{\lambda_2}{\omega^2} \cos(2s\Theta_+) \cos(2s\Theta_-) - \frac{4\lambda_1}{\omega^2} \cos(s\Theta_+) \cos(s\Theta_-) + \frac{\lambda_3}{2\omega^2} \cos(2s\Theta_+ + \phi)$$

with flips $\Theta_\pm \rightarrow \pi - \Theta_\pm$ at $\Theta_+ = \pi$ for $f_y(t) = \lambda_1 \cos(\omega t) + \lambda_2 \cos(2\omega t)$ and $f_{y-x}(t) = -\lambda_3 \cos(2\omega t + \phi)$

- H_{eff} describes a particle moving on the Möbius strip in the presence of a non-separable lattice potential

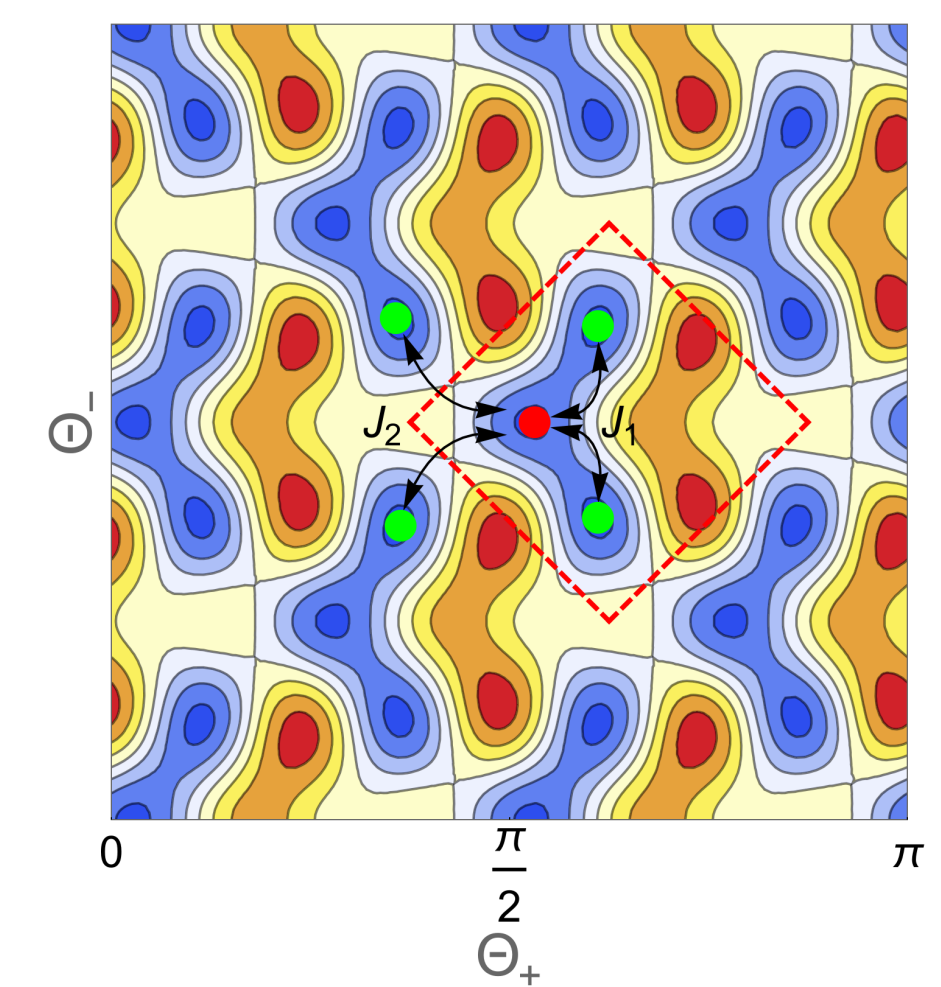


Tightly bounded particle in the asymmetric Lieb lattice

- quantum description in resonant Hilbert subspace

$$H_{\text{eff}} = -J_1 \sum_{ij} \hat{a}_i^\dagger \hat{a}_j - J_2 \sum_{i'j'} \hat{a}_{i'}^\dagger \hat{a}_{j'}$$

- for $J_2/J_1 \ll 1$, eigenvalues of H_{eff} form well separated three bands where the central band is flat



Ultra-cold bosonic atoms in the flat band

- N bosons interact via Dirac-delta potential $g_0 \delta(\mathbf{r})$

- many-body Floquet Hamiltonian restricted to the flat band subspace

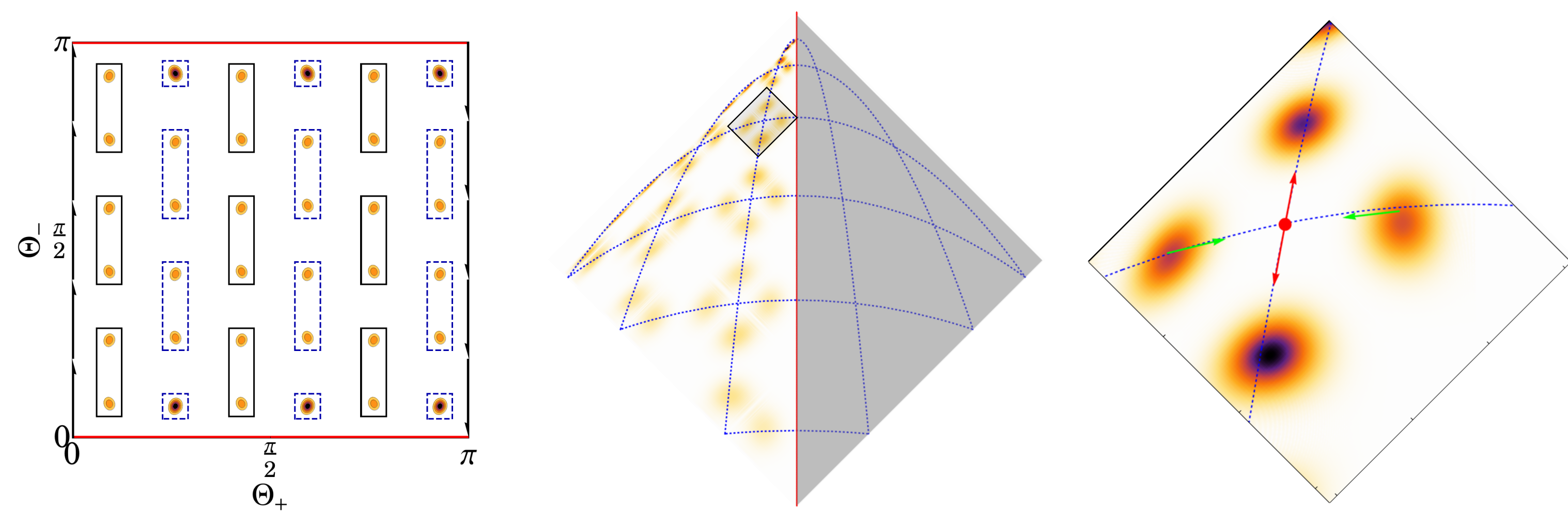
$$\hat{\mathcal{H}} = \frac{1}{sT} \int_0^{sT} dt \int dx dy \hat{\psi}^\dagger \left[H - i\partial_t + \frac{g_0}{2} \hat{\psi}^\dagger \hat{\psi} \right] \hat{\psi} \approx \sum_{ijkl} U_{ijkl} \hat{b}_i^\dagger \hat{b}_j^\dagger \hat{b}_k \hat{b}_l + \text{const}$$

- $\hat{\psi} \approx \sum_{i=1}^{s(s+1)/2} w_i \hat{b}_i$ with the bosonic operators $[\hat{b}_i, \hat{b}_j^\dagger] = \delta_{ij}$

- control of the contact interactions by changes of scattering length using Feshbach resonance mechanism

$$U_{ijkl} = \frac{1}{sT} \int dt \int dx dy g_0(t) w_i^* w_j^* w_k w_l$$

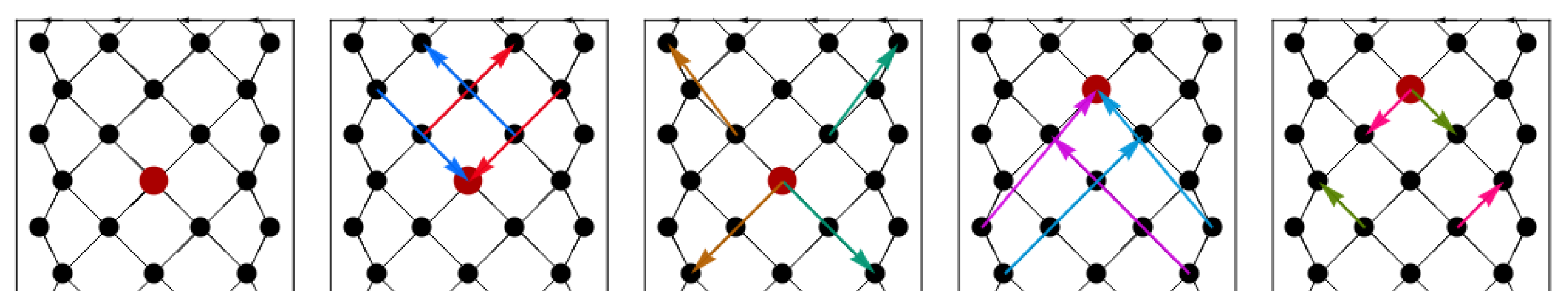
- Wannier states corresponding to the flat band $w_i(x, y, t) = w_i(x, y, t + sT)$



Pair tunnelling processes

- hard-core bosons Floquet Hamiltonian

$$H_F = V \sum_{\langle ij \rangle} \hat{n}_i \hat{n}_j - J \sum_{\langle\langle ijkl \rangle\rangle} \left(\hat{b}_i^\dagger \hat{b}_j^\dagger \hat{b}_k \hat{b}_l + H.c. \right) \quad \hat{n}_i = \hat{b}_i^\dagger \hat{b}_i$$



- simultaneous tunneling of two particles between four distinct lattice sites $J = 4U_{ijkl}|_{\{i \neq j \neq k \neq l\}}$
- nearest neighbour repulsion $V = 4U_{ijij}$

References

- [1] K. Sacha, Sci. Rep. 5, 10787 (2015).
- [2] K. Giergiel, A. Dauphin, M. Lewenstein, J. Zakrzewski, and K. Sacha, NJP 21, 052003 (2019).
- [3] A. Kosior and K. Sacha, Phys. Rev. A 97, 053621 (2018).
- [4] K. Giergiel, A. Kuroś, and K. Sacha, Phys. Rev. B 99, 220303 (2019).
- [5] P. Matus and K. Sacha, Phys. Rev. A 99, 033626 (2019).
- [6] S. Taic, H. Ozawa, T. Ichinose, T. Nishio, S. Nakajima, and Y. Takahashi, Science Advances 1 (2015).
- [7] K. Giergiel, A. Miroszewski, and K. Sacha, Phys. Rev. Lett. 120, 140401 (2018).

**Resonating valence bond
realization of spin-1 non-Abelian
chiral spin liquid on the torus**

Hua-Chen Zhang

Resonating valence bond
realization of spin-1 non-Abelian
chiral spin liquid on the torus

Hua-Chen Zhang @
IOP CAS & TU Dresden
23 Feb 2021, Benasque SCS

- We propose resonating valence bond (RVB) wave functions for a spin-1 lattice system on the torus that realize a non-Abelian chiral spin liquid.
- These wave functions are shown to be equivalent to chiral correlation functions in a certain conformal field theory (CFT) and identified to be a lattice analogue of the bosonic Moore-Read state at unit filling.
- The topological order of this system is revealed by explicit construction of the topologically degenerate ground states and analytical computation of their modular matrices.

Simulation of three-dimensional quantum systems with projected entangled-pair states

Patrick Vlaar

Simulation of three-dimensional quantum systems with projected entangled-pair states

Patrick Vlaar & Philippe Corboz

arXiv:2102.06715



UNIVERSITY OF AMSTERDAM
Institute of Physics

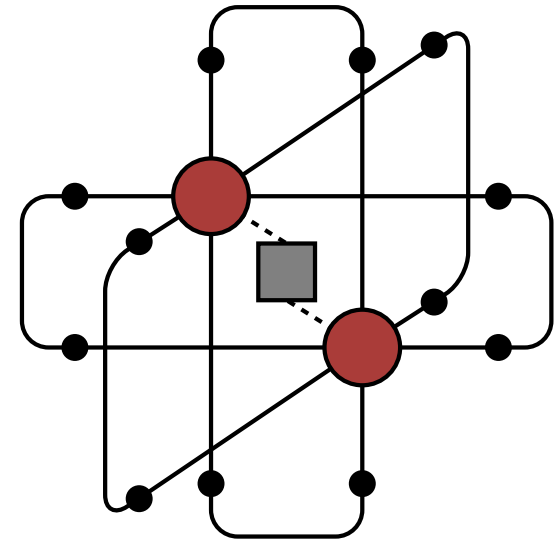


European Research Council

Established by the European Commission

Simulation of three-dimensional quantum systems with projected entangled-pair states

- Tensor network techniques very successful in 1D and 2D, however applications in 3D are limited
- We present two techniques
 - Cluster contraction
 - Full contraction
- We expect this work to be an important step towards making iPEPS a promising tool to study open problems in 3D



Solving frustated Ising models using tensor networks

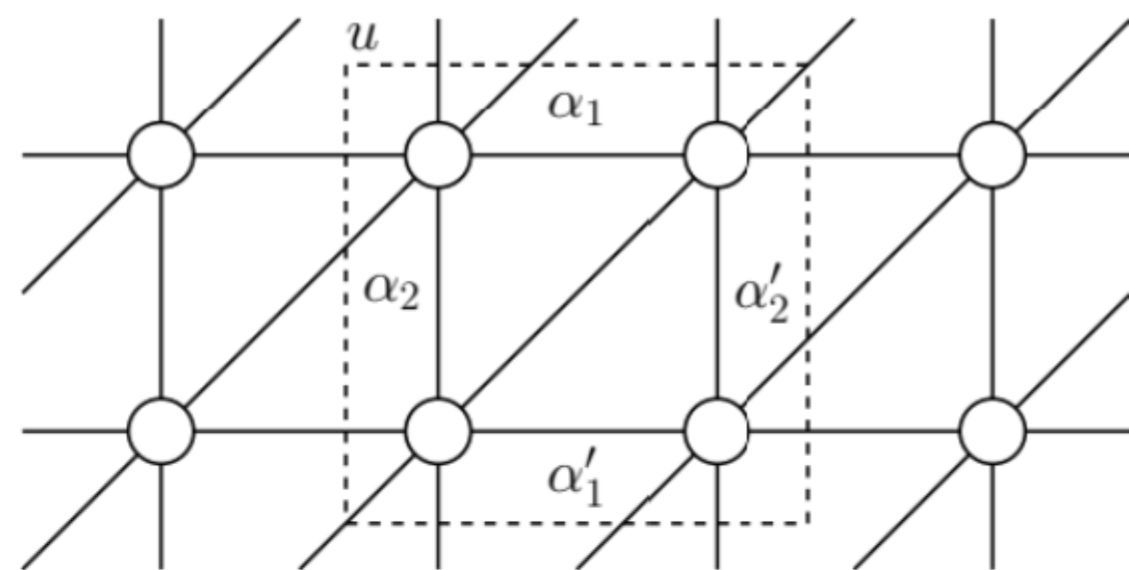
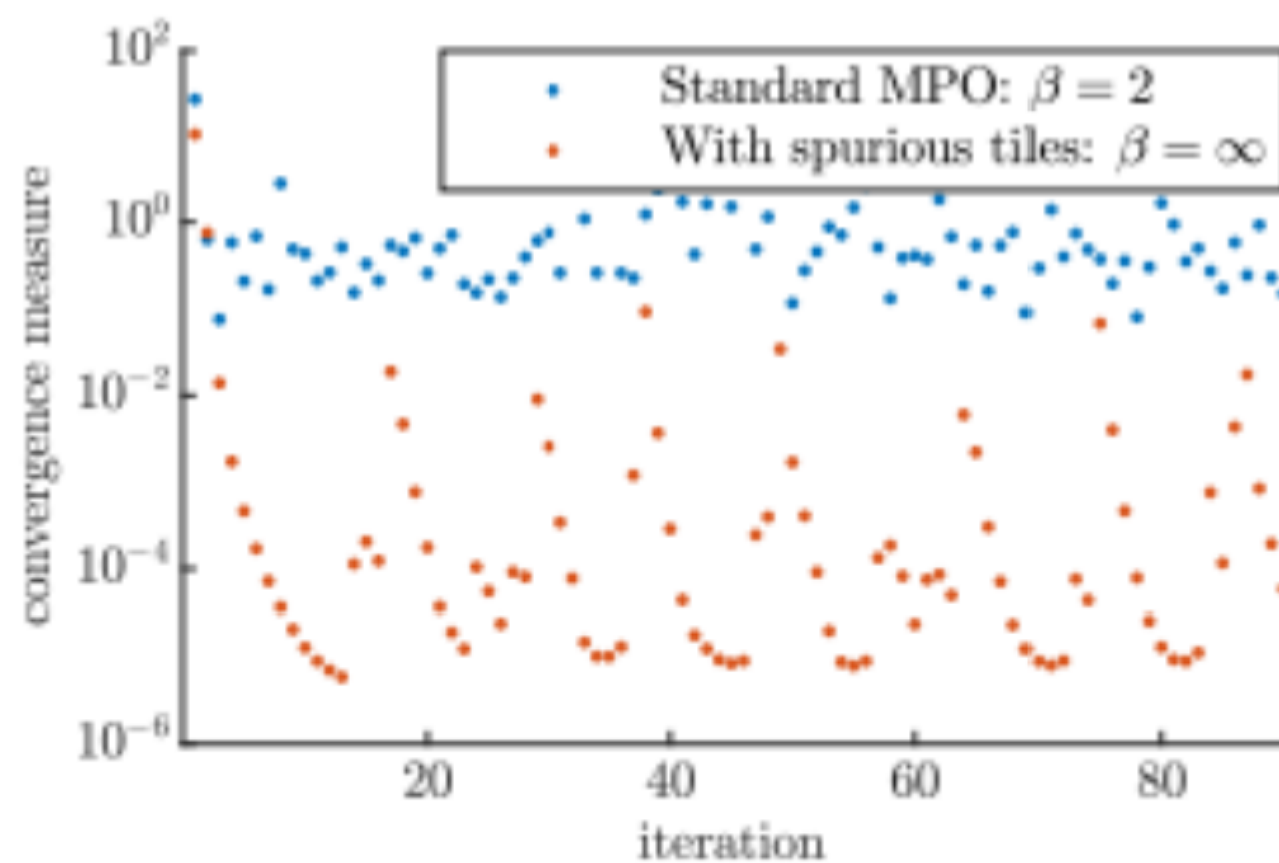
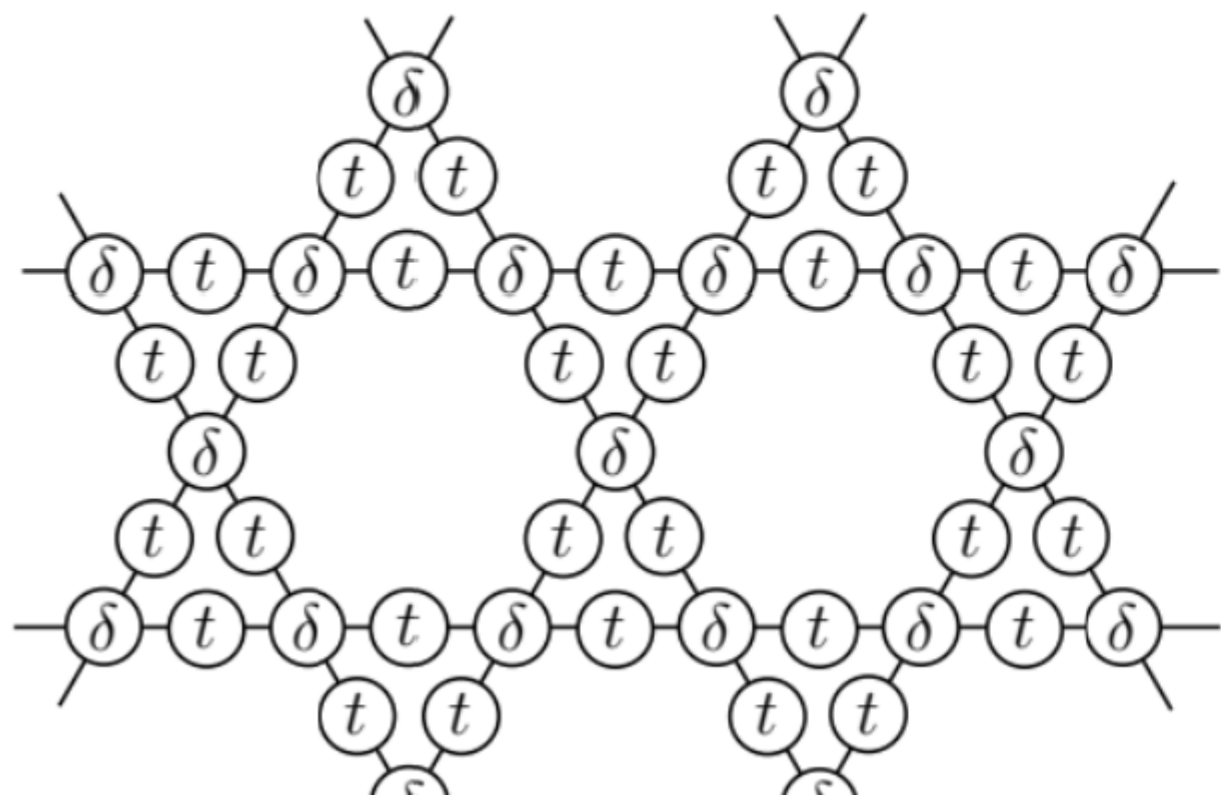
Bram Vanhecke

Solving frustrated Ising models using tensor networks

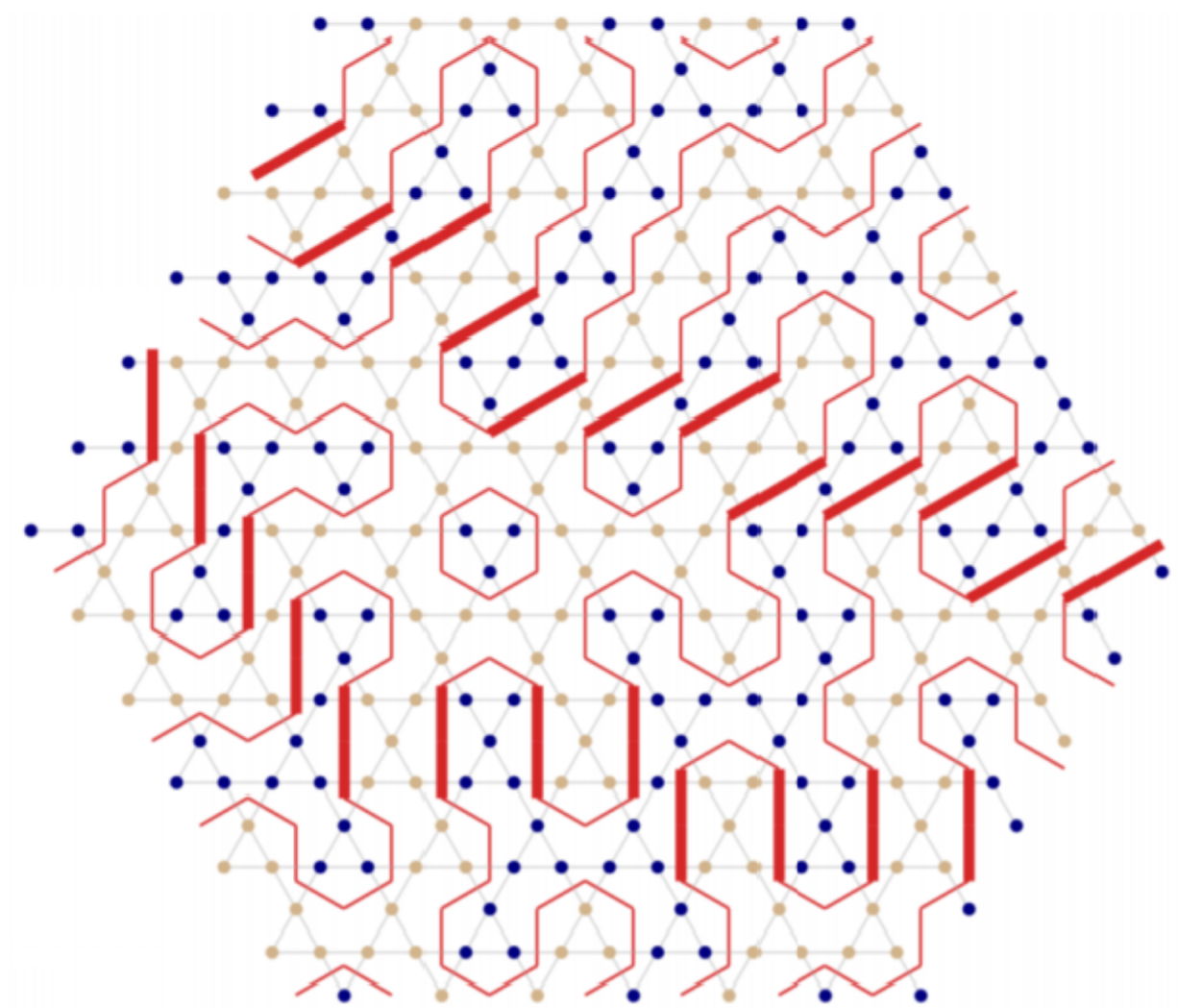
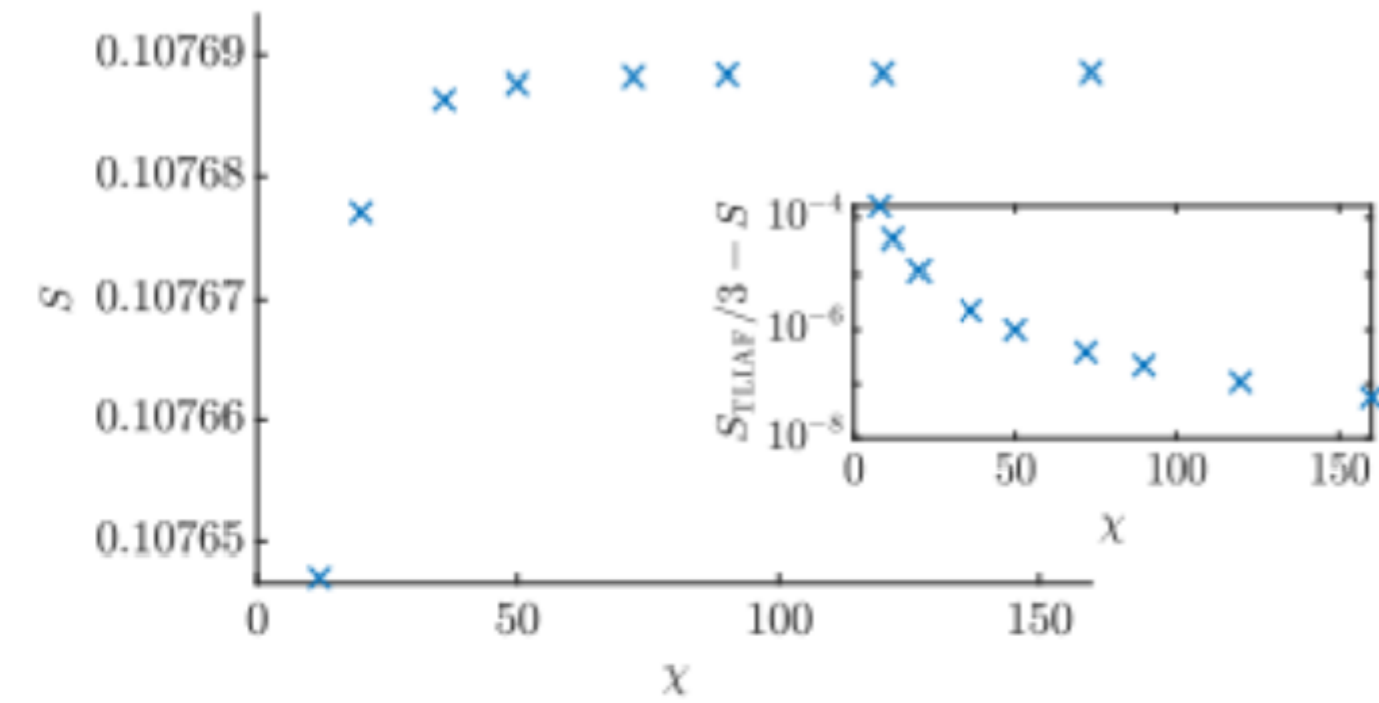
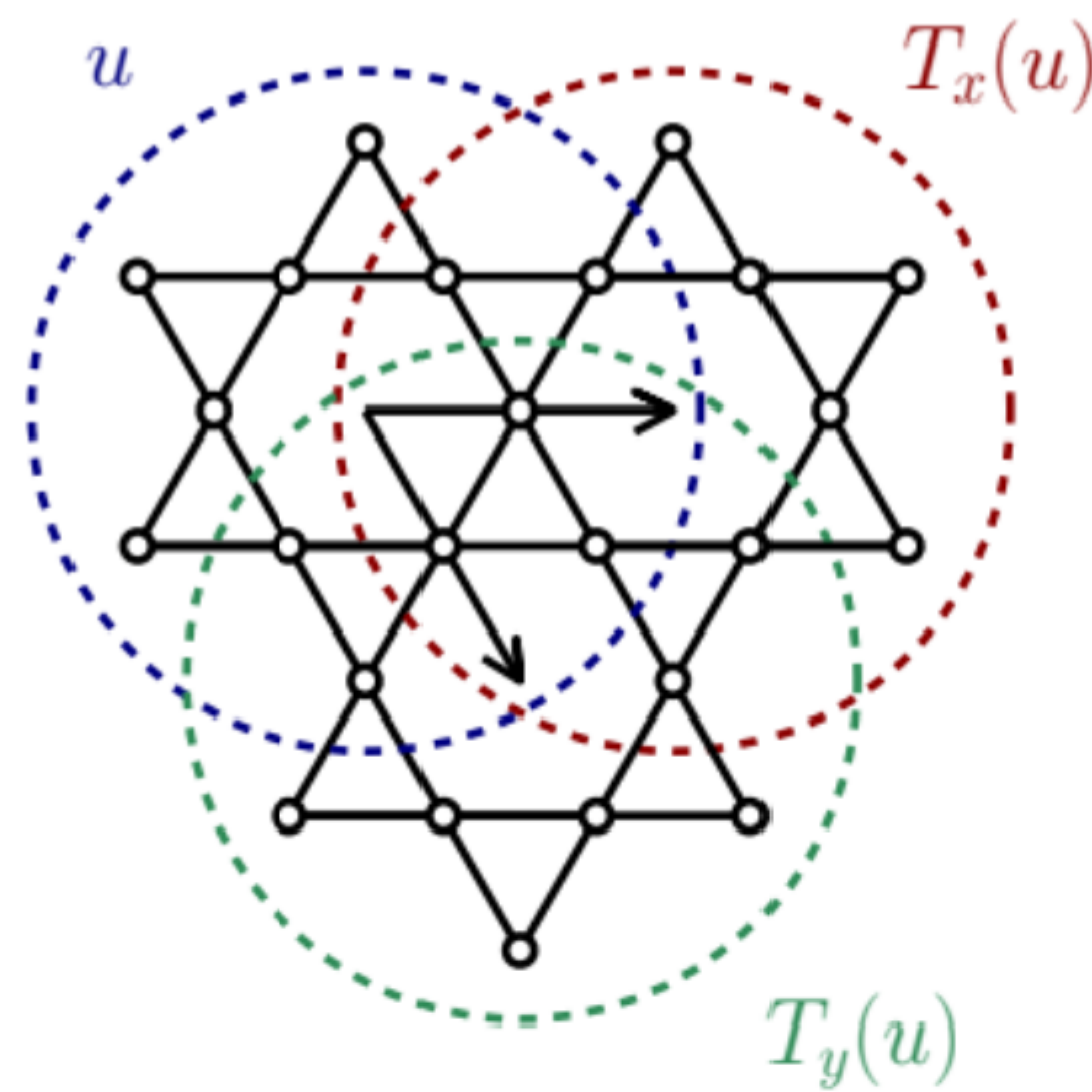
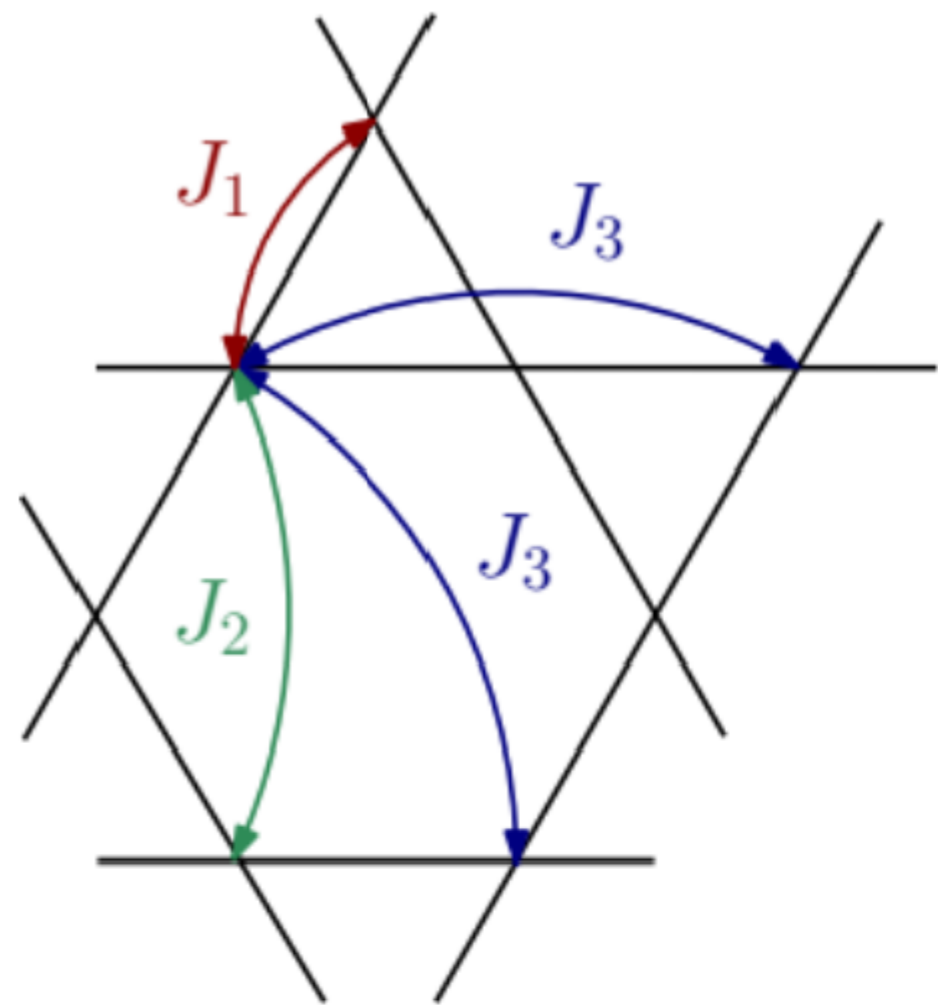
Bram Vanhecke, Jeanne Colbois, Laurens Vanderstreaten, Frank Verstraete, Frédéric Mila

Phys. Rev. Research 3, 013041 – Published 13 January 2021

	AF-Ising on kagome	AF-Ising on triangular
MPS	0.5018331646 ($D = 10$)	0.3230659407 ($D = 250$)
exact	0.5018331646	0.3230659669



Spurious cluster configurations



Convex sets, and linear programming: $A\vec{x} \leq \vec{B}$

String order parameters for symmetry fractionalization in an enriched toric code

Mohsin Iqbal

String order parameters for symmetry fractionalization in an enriched toric code

José Garre-Rubio, Mohsin Iqbal, David T. Stephen

arXiv:2011.02981

SCS Benasque-2021

Goal

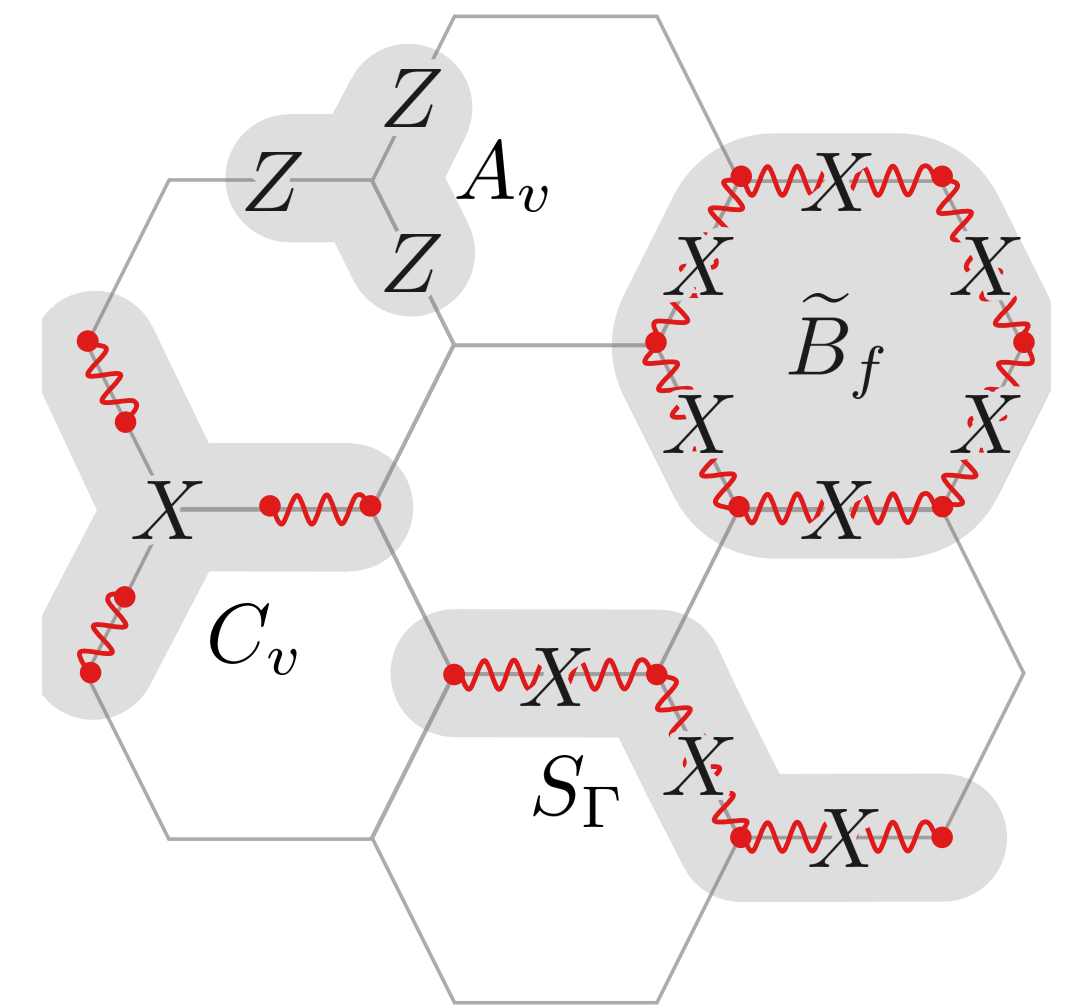
**Construct SOP for characterizing the symmetry fractionalization pattern of the anyons:
detect the SET phase**

We start from TC on edges decoupled from
ferromagnet on vertices

$$\tilde{H}_{TC} = H_{TC} - \sum_{v \in V} X_v$$

$$H_{SET} = - \sum_{v \in V} A_v - \sum_{f \in F} \tilde{B}_f - \sum_{v \in V} C_v \frac{1 + A_v}{2}$$

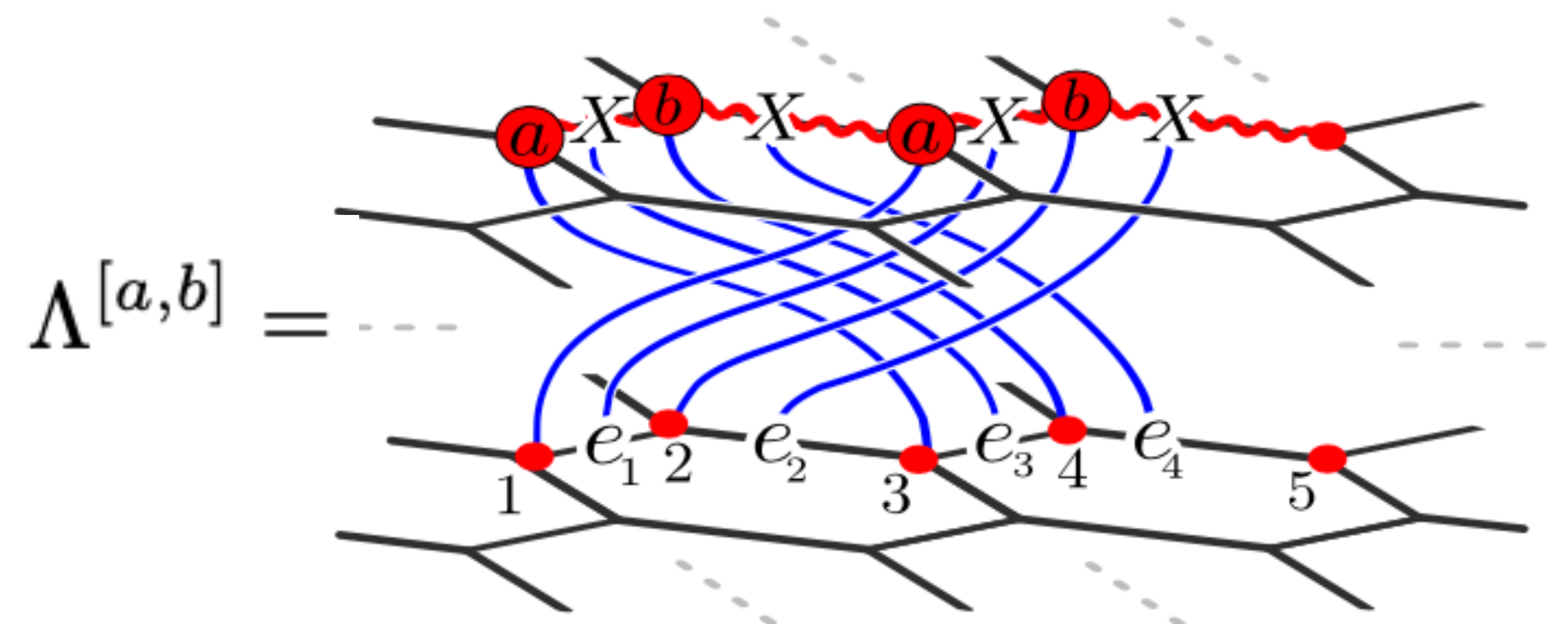
We end in a decorated TC
with cluster states



The charge fractionalizes TRS, BC inversion and the on-site symmetry $\mathbb{Z}_2 \times \mathbb{Z}_2$

We generalize the SOP of [1] beyond PEPS and RGFP to measure the SF class of the charge.

$$\mathcal{O}^{[a,b]} = \frac{\langle \Lambda^{[a,b]} \rangle}{\langle \Lambda^{[0,0]} \rangle}$$



Results

📌 Test the SOP in the Hamiltonian interpolation

$$\lambda \tilde{H}_{TC} + (1 - \lambda) H_{SET}$$

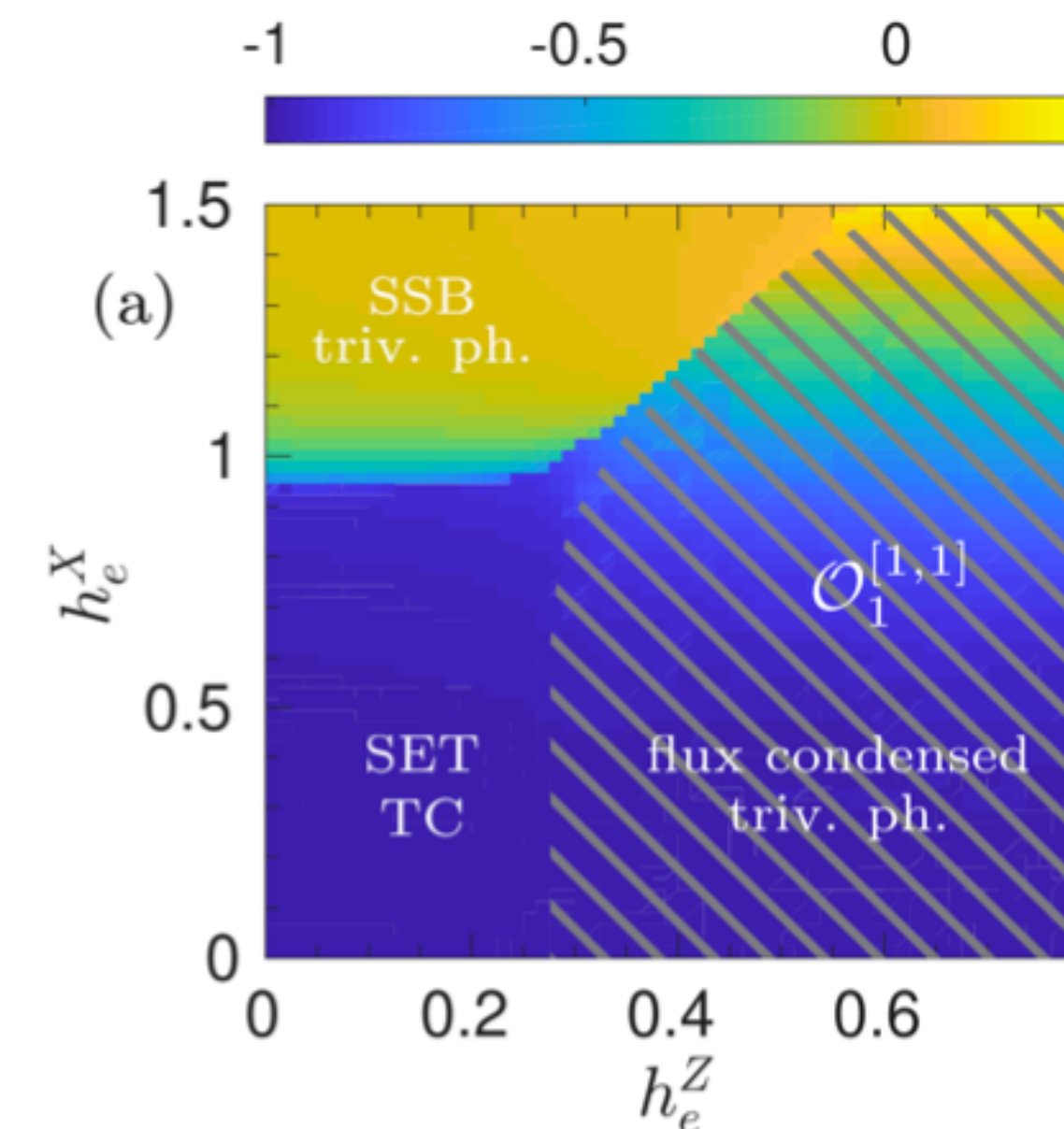
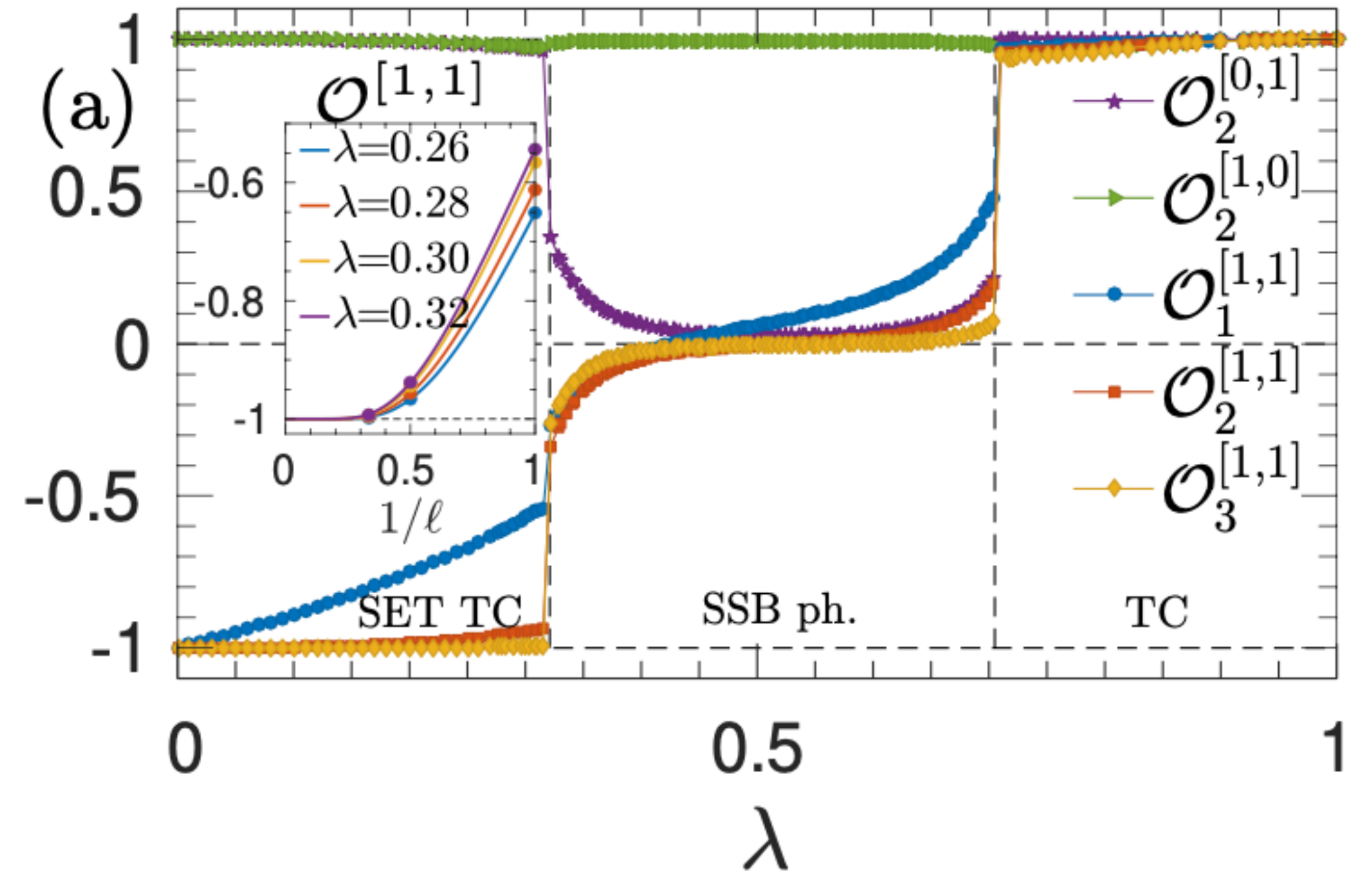


📌 Phase diagram under magnetic fields

$$H_{SET} - h_e^X \sum_e Z_e - h_e^Z \sum_e X_e$$

★ We observe SSB because of the condensation of the anyon that fractionalizes the symmetry (charge vs flux)

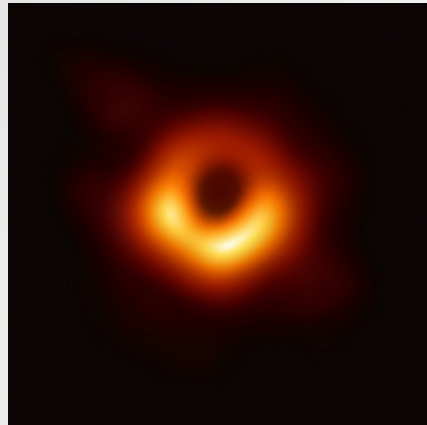
★ The phase diagram changes from the one of the TC: infinite line between trivial (topological) phases!



The SYK model from strained honeycomb irridates: A case study

Mikael Fremling

The SYK model from strained honeycomb iridates



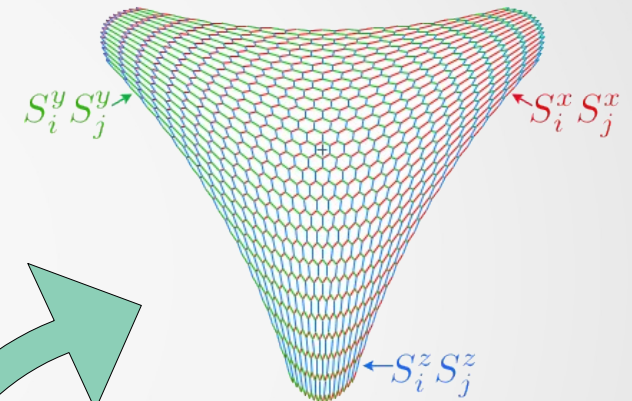
The dream

Sachdev-Ye-Kitaev

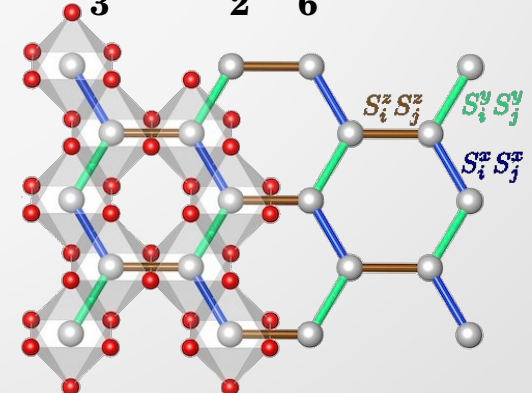


SYK

Strained
Kitaev Honeycomb



$\text{H}_3\text{LiIr}_2\text{O}_6$ Iridates

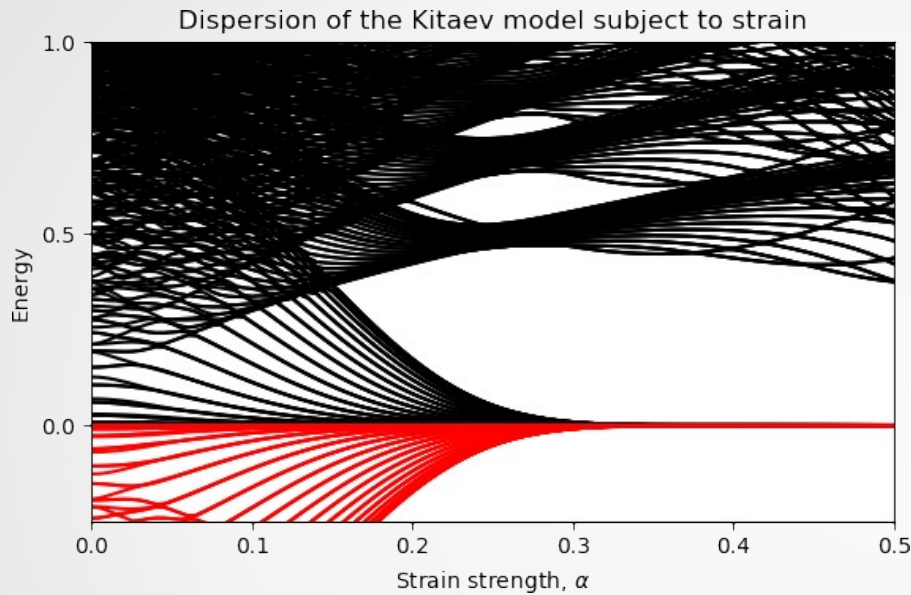


Mikael Fremling

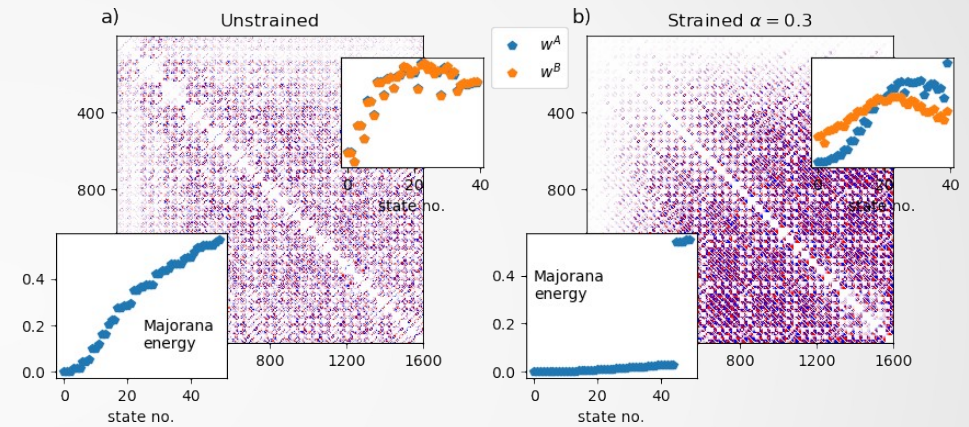
Utrecht University



Random hopping elements in a flat band

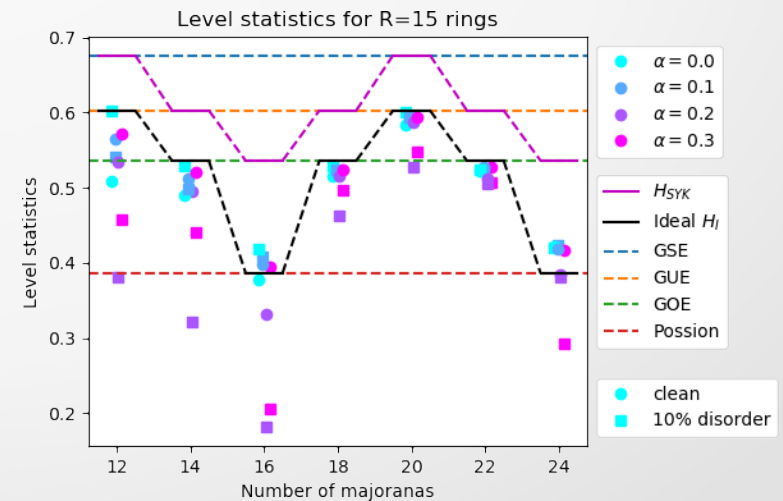


Interaction elements are random



$$H_{SYK} = \sum_{i,j,k,l} J_{i,j,k,l} \gamma_i \gamma_j \gamma_k \gamma_l$$

$$H_{Strain} = \sum_{n_1, n_2; m_3, m_4} J_{n_1, n_2; m_3, m_4} \gamma_{n_1}^A \gamma_{n_2}^A \gamma_{m_3}^B \gamma_{m_4}^B$$

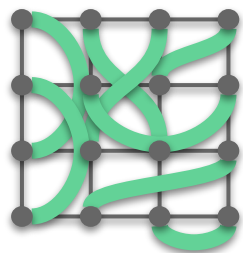


Variational wave functions for spin-phonon models

F. Ferrari

Variational wave functions for **spin-phonon** models

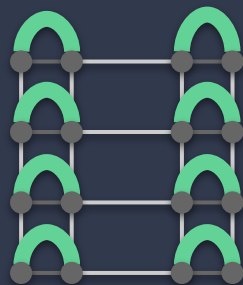
Francesco Ferrari, Federico Becca, Roser Valentí



spin liquid

?

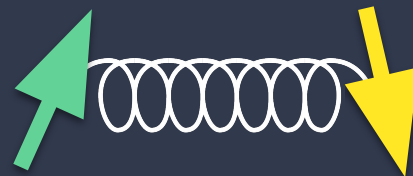
valence-bond order



magnetoelastic coupling
 $J[1 + g(X_1 - X_2)]\mathbf{S}_1 \cdot \mathbf{S}_2$

variational Ansätze

$|\Psi_{\text{spin-phonon}}\rangle$



quantum phonons
 $\frac{\omega}{2}(P^2 + X^2)$

Monte Carlo sampling